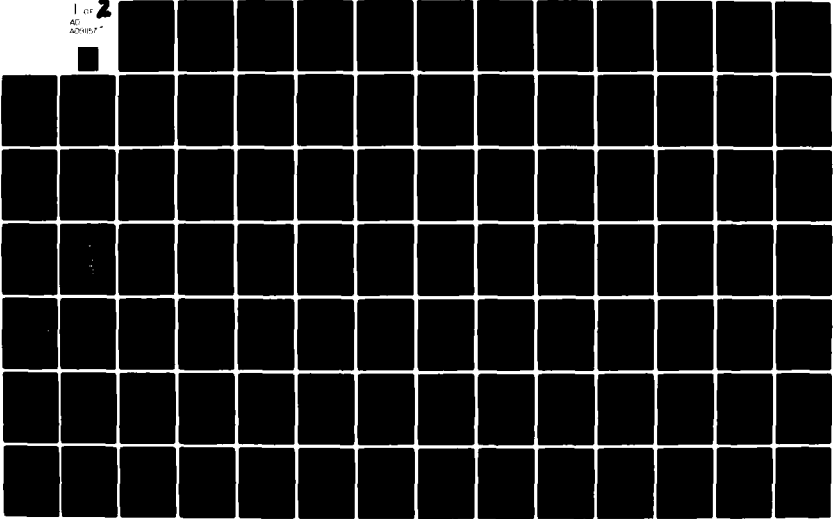


AD-A091 157

PENNSYLVANIA STATE UNIV UNIVERSITY PARK APPLIED RESE--ETC F/G 14/2
DEVELOPMENT OF A FAST-RESPONSE TOTAL PRESSURE PROBE FOR USE IN --ETC(U)
OCT 79 J A SPIVAK N00014-75-C-1143
ARL/PSU-TM-79-182 NL

UNCLASSIFIED

1 of 2
AD A091157



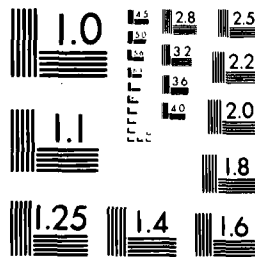
1

OF



AD-

A091157



MICROCOPY RESOLUTION TEST CHART
NATIONAL BUREAU OF STANDARDS-1963-A

AD A091157

z

12

LEVEL

DEVELOPMENT OF A FAST-RESPONSE TOTAL PRESSURE
PROBE FOR USE IN AN AXIAL FLOW FAN

J. A. Spivak

Technical Memorandum
File No. 79-182
22 October 1979
Contract No. N00014-75-C-1143

Copy No. 8

The Pennsylvania State University
APPLIED RESEARCH LABORATORY
Post Office Box 30
State College, PA 16801

NAVY DEPARTMENT
NAVAL SEA SYSTEMS COMMAND

Approved for Public Release
Distribution Unlimited

SDTIC
ELECTED
NOV 3 1980

DDG FILE COPY

80 11 03 233

14

UNCLASSIFIED

SECURITY CLASSIFICATION OF THIS PAGE (When Data Entered)

REPORT DOCUMENTATION PAGE		READ INSTRUCTIONS BEFORE COMPLETING FORM
1. REPORT NUMBER 79-182	2. GOVT ACCESSION NO. AD-A091157	3. RECIPIENT'S CATALOG NUMBER
4. TITLE (and Subtitle) DEVELOPMENT OF A FAST-RESPONSE TOTAL PRESSURE PROBE FOR USE IN AN AXIAL FLOW FAN.	5. TYPE OF REPORT & PERIOD COVERED Technical Memorandum	6. PERFORMING ORG. REPORT NUMBER
7. AUTHOR(S) J. A. Spivak	8. CONTRACT OR GRANT NUMBER(s) N00014-75-C-1143	
9. PERFORMING ORGANIZATION NAME AND ADDRESS Applied Research Laboratory Post Office Box 30 State College, PA 16801	10. PROGRAM ELEMENT, PROJECT, TASK AREA & WORK UNIT NUMBERS	
11. CONTROLLING OFFICE NAME AND ADDRESS Naval Sea Systems Command Department of the Navy Washington, DC 20362	12. REPORT DATE 22 Oct 1979	13. NUMBER OF PAGES 91
14. MONITORING AGENCY NAME & ADDRESS (if different from Controlling Office) 96	15. SECURITY CLASS. (of this report) UNCLASSIFIED	15a. DECLASSIFICATION/DOWNGRADING SCHEDULE
16. DISTRIBUTION STATEMENT (of this Report) Approved for public release. Distribution unlimited. Per NAVSEA -		
17. DISTRIBUTION STATEMENT (of the abstract entered in Block 20, if different from Report)		
18. SUPPLEMENTARY NOTES		
19. KEY WORDS (Continue on reverse side if necessary and identify by block number) pressure, probe, design, calibration, unsteady, flows, turbomachinery This		
20. ABSTRACT (Continue on reverse side if necessary and identify by block number) The development of a fast-response total pressure probe is presented. This probe is intended for use in the study of unsteady flows in turbomachines. Emphasis is on the design and calibration of this probe, which utilizes a temperature-compensated transducer to obtain both the AC and DC components of the fluctuations. A description of the calibration procedure and calibration device, a Galton Whistle, employed to determine the time-dependent response of this probe is presented. In addition, typical data demonstrating the use of this probe in an axial flow fan are discussed.		

DD FORM 1 JAN 73 1473 EDITION OF 1 NOV 68 IS OBSOLETE

UNCLASSIFIED

SECURITY CLASSIFICATION OF THIS PAGE (When Data Entered)

391 007

ABSTRACT

The development of a fast-response total pressure probe is presented. This probe is intended for use in the study of unsteady flows in turbomachines. Emphasis is on the design and calibration of this probe, which utilizes a temperature-compensated transducer to obtain both the AC and DC components of the fluctuations. A description of the calibration procedure and calibration device, a Galton Whistle, employed to determine the time-dependent response of this probe is presented. In addition, typical data demonstrating the use of this probe in an axial flow fan are discussed.

Accession For	
NTIS GRA&I	<input checked="" type="checkbox"/>
DTIC TAB	<input type="checkbox"/>
Unannounced	<input type="checkbox"/>
Justification	
By _____	
Distribution/ _____	
Availability Codes	
Dist	Avail and/or Special
A	

TABLE OF CONTENTS

	<u>Page</u>
ABSTRACT	iii
LIST OF FIGURES	vi
LIST OF TABLES	viii
NOMENCLATURE	ix
ACKNOWLEDGMENTS	x
I. INTRODUCTION	1
PREVIOUS STUDIES	2
Modeling of Total Pressure Probes	2
Time-Averaged Pressure Measurement in an Unsteady Flow	5
Unsteady Flow Fluctuating Total Pressure Measurements	6
SCOPE OF THE INVESTIGATION	8
II. PROBE DESIGN CONSIDERATIONS AND CONSTRUCTION	10
AERODYNAMIC REQUIREMENTS	10
FREQUENCY RESPONSE REQUIREMENTS	11
MECHANICAL REQUIREMENTS	11
PROBE DESIGN AND CONSTRUCTION	12
Probe	12
Pressure Transducer	14
III. PROBE TESTING	17
STATIC TESTS	17
Reynolds Number and Yaw and Pitch Angle Calibration	20
Static Sensitivity Calibration	25
DYNAMIC TESTS	25
Probe Calibration	31

	<u>Page</u>
IV. RESEARCH FACILITY	36
AXIAL FLOW RESEARCH FAN	36
FLOW MEASURING INSTRUMENTATION	38
V. PROBE APPLICATION	43
DATA ACQUISITION	43
DATA REDUCTION	59
DISCUSSION AND PRESENTATION OF RESULTS	52
VI. SUMMARY AND CONCLUSIONS	64
VII. RECOMMENDATIONS FOR FURTHER RESEARCH	67
REFERENCES	68
APPENDIX A: THEORETICAL AND EXPERIMENTAL EVALUATION OF TUBE/CAVITY SYSTEM RESPONSE	71
APPENDIX B: MISCELLANEOUS CALIBRATION DATA	79

LIST OF FIGURES

<u>Figure</u>	<u>Title</u>	<u>Page</u>
1	Generalized Tube/Cavity System	3
2	Fast-Response Kiel Probe	13
3	Pressure Transducer: (a) Transducer Detail, (b) Bridge Circuitry	15
4	Open Jet Facility	18
5	Probe Holding Device Showing Yaw/Pitch Mechanism	19
6	Schematic of the Static Test Setup	21
7	Yaw/Pitch Angle Definition	22
8	Reynolds Number Calibration Curves: (a) Standard Kiel Probe, (b) Fast-Response Kiel Probe	23
9	Yaw/Pitch Angle Calibration Curves: (a) and (c) Standard Kiel Probe, (b) and (d) Fast-Response Kiel Probe	24
10	Fast-Response Kiel Probe Static Sensitivity Calibration Curve	26
11	Basic Galton Whistle Configuration	28
12	Galton Whistle Response Curve	30
13	Galton Whistle, Showing the Fast-Response Kiel Probe's Simulator and the Reference Transducer Mounted at a Typical Location	32
14	Schematic of the Dynamic Calibration Setup	33
15	Close-up of the Fast-Response Kiel Probe's Simulator	34
16	Frequency Response Curves of the Fast-Response Kiel Probe's Simulator	35
17	Axial Flow Research Fan	37
18	Schematic of the Flow Measurement Instrumentation	39

<u>Figure</u>	<u>Title</u>	<u>Page</u>
19	Four-Cycle Distortion Generating Screen	45
20	The Effect on a Typical Probe Output of Increasing the Number of Ensemble-Averaged Periods	46
21	Probe Orientation Parameters: (a) Circumferential Angle, (b) Yaw Angle, (c) Axial and Radial Locations	47
22	Spectral Content of a Typical Fast-Response Kiel Probe Output for One Rotor Revolution	53
23	Periodic Variation of the Ensemble-Averaged Total Pressure Coefficient, Uncorrected for Probe Dynamic Response, Test Condition No. 1	54
24	Periodic Variation of the Ensemble-Averaged Total Pressure Coefficient and the Time-Averaged Value of the Standard Kiel Probe, Test Condition No. 1	55
25	Periodic Variation of the Ensemble-Averaged Total Pressure Coefficient and the Time-Averaged Value of the Standard Kiel Probe, Test Condition No. 2	57
26	Periodic Variation of the Ensemble-Averaged Total Pressure Coefficient and the Time-Averaged Value of the Standard Kiel Probe, Test Condition No. 3	60
27	Axial Velocity Distribution Just Upstream of Rotor for Four-Cycle Screen ($V_{AVG} = 56$ ft/sec)	61
28	Schematic of Four-Cycle Flow Distortion Showing Probe Position Relative to Flow	62
B-1	Static Calibration of Transducer T-1	80
B-2	Rerun of Reynolds Number Calibration for the Standard Kiel Probe	81
B-3	Calibration Data Relating V_{AVG} and Casing Static Pressure for a Four-Cycle Distorted Inflow at R_{MEAN}	82
B-4	Static Calibration of Transducer T-2	83

LIST OF TABLES

<u>Table</u>	<u>Title</u>	<u>Page</u>
1	Transducer Specifications	16
2	Test Conditions	44
3	Comparison of the Time-Averaged Total Pressures for Test No. 1 and Test No. 2	59

NOMENCLATURE

<u>Symbol</u>	<u>Definition</u>
AC	fluctuating pressure component
a_n, b_n	Fourier coefficients of n^{th} harmonic
C_{p_t}	pressure coefficient
DC	time-averaged pressure component
f	frequency (Hz)
P_T	total pressure (psfg)
P_S	static pressure (psfg)
P_{ATM}	atmospheric pressure (psf)
R_{MEAN}	AFRF mean radius (inches)
R_{HUB}	AFRF hub radius (inches)
t	time
U	rotor blade speed at R_{MEAN} (fps)
V_{AVG}	circumferential-mean inlet axial velocity (fps)
V_x	inlet axial velocity (fps)
ρ	density (slugs/ft ³)
θ_C	circumferential probe position (degrees)
θ_P	probe yaw angle (degrees)

ACKNOWLEDGMENTS

The author would like to express his thanks to his research advisor, Dr. Robert E. Henderson, for his help and guidance throughout the project. The technical assistance given by Messrs. Edgar P. Bruce, Wilden L. Nuss, George M. Sayers, and Robert W. Woods is also appreciated.

This project was conducted at the Garfield Thomas Water Tunnel of the Applied Research Laboratory at The Pennsylvania State University. Financial support for the investigation was provided by Project SQUID, Contract No. 8960-4. Project SQUID is a cooperative program of basic research relating to jet propulsion. It is sponsored by the Office of Naval Research and is administered by Purdue University through Contract N00014-75-C-1143, NR-089-038.

CHAPTER I

INTRODUCTION

Modern turbomachine design procedures rely on an axisymmetric steady flow model as a basis for their design because information to date concerning the unsteady flow process is largely inadequate. A satisfactory method of measuring unsteady flow parameters would provide valuable data contributing to the improved design of many turbomachines, which would in turn lead to higher efficiencies and less structural vibration. Further efforts in the improvement of turbomachine design will depend largely on the continued investigation and understanding of the actual unsteady flow phenomena involved.

The purpose of this investigation is to develop a fast-response total pressure probe to aid in the description of the unsteady flow field in an axial fan stage by permitting the measurement of the instantaneous total pressure. This probe will complement instruments already available for use in the Axial Flow Research Fan (AFRF) at the Applied Research Laboratory, The Pennsylvania State University, to determine the spatial velocity distribution (1), the unsteady blade surface pressures (2), and lift and pitching moment (3) present on the blades of an axial flow fan stage. The need now is to add to these unsteady measurements the capability to determine the details of the total pressure field, including not only the time-averaged total pressure but also its instantaneous fluctuations. The design, construction, and calibration of such a probe is the primary purpose of this study.

PREVIOUS STUDIES

Modeling of Total Pressure Probes. In the design of a probe that will measure time-dependent pressures, one must obtain beforehand a knowledge of its response characteristics. This will, in general, depend on the probe's internal geometry and size and on the response of any other components used in conjunction with the probe. Developments over the past few years have made it possible to produce pressure transducers of high quality at a miniaturized scale (~0.1 inch in diameter), small enough to be housed in the probe itself. These transducers have a sufficiently high first resonant frequency (40 to 200 kHz) to make them applicable to most flow studies. From a response viewpoint, direct contact of transducer and flow is the ideal configuration. However, directional velocity sensitivity, sampling size of the transducer, and protection of the transducer itself would warrant installation of the transducer in a fixed volume as generalized in Figure 1. These aspects will be considered when probe design requirements are discussed.

Modeling of the generalized tube/cavity system shown in Figure 1 has been approached in various ways. Taback (4) used an electro-mechanical analogy based on the transmission characteristics of electrical lines to predict the response of a pressure measuring system to a sinusoidal input. System frequency response and phase shift were obtained from the velocity of propagation in tubes calculated from the Rayleigh formula (5), combined with experimentally measured values of attenuation. The dependence of this model on experimental values severely limits its applicability.

Linear, second-order models have been developed in many textbooks. The basis for these models is the analog between the mechanical system

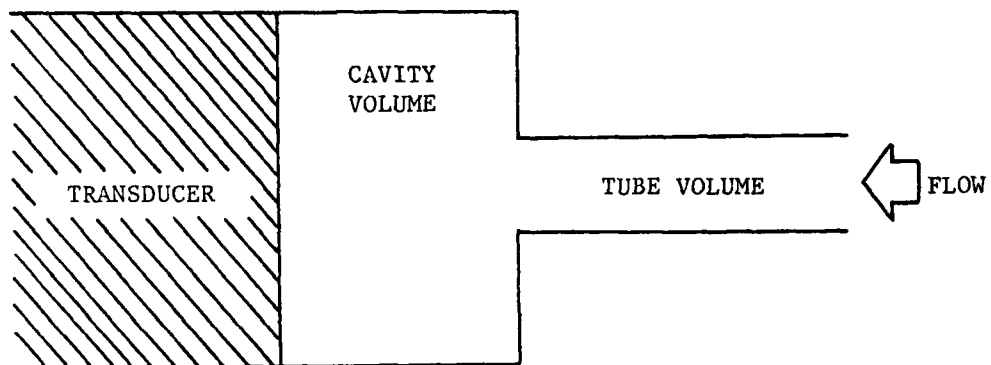


FIGURE 1. GENERALIZED TUBE/CAVITY SYSTEM

of a mass on a massless spring and the fluid system (having the same mass) consisting of the fluid in the tube of a resonator and the cavity volume. Holman (6) uses a Helmholtz resonator to model the system. The resonant frequency is readily obtainable from the model's basic equation of motion. Doeblein (7) uses a simplified energy analysis to the same end.

Delio et al. (8) treated the tube/cavity arrangement as a lumped parameter system, with fluid properties constant along the tube length, assuming the amplitudes of the disturbances were small. What was obtained was a second-order model that became nonlinear for large disturbances. This model, as well as other second-order models, loses its accuracy for small volumes and tubing radii due to nonlinear viscous friction effects.

An extended theory, based on the motion of fluid particles inside a resonator, was reported by Alster (9). The resonant frequency was found to be dependent on the shape of the cavity in question. Formulas for specific shapes (spherical, conical, frustrum of a cone, cylindrical prism, and quarter wave) were derived. Alster's theory treated the resonances of Helmholtz resonators and quarter wavelength resonators together (considered only separately until then). The results of his calculations were verified with high accuracy.

A study of the application of Delio's lumped parameter system, the Helmholtz oscillator model, and Alster's method in the design of fast-response total pressure probes was conducted by Atkins (10, 11). Theoretical model predictions were compared with experimental values up to a frequency of 10 kHz. Atkins' results show that all of the models

disagree somewhat with experiment, with significant differences existing between the Helmholtz model and Alster's method.

Nonlinear analyses, based on the Navier-Stokes equations and equations of continuity, energy, and state, are developed by Iberall (12) and Bergh and Tijdeman (13). Small sinusoidal pressure variations, laminar flow throughout the system, and a geometrically long system compared to the radius of any tube in the system were some of the assumptions made. Iberall's analysis was restricted to a single tube/cavity system, while Bergh and Tijdeman's model extended the theory to cover a series connection of any number of tubes and cavities. Experimental comparisons with theory up to 300 Hz were conducted in Reference (10), with results indicating a high precision of prediction.

Nyland, Englund, and Anderson (14) confirmed the value of the above analyses by using the equations of Bergh and Tijdeman and Iberall in the frequency range up to 5,000 Hz. In addition, they developed a computer program for the multiple tube/cavity analysis of Bergh and Tijdeman.

Based on the preceding literature, it would seem that any of the models would be suitable for predicting probe response, noting the assumptions and limitations of each model. The Helmholtz model would seem most suitable for a quick check on the resonant frequency, with Bergh and Tijdeman's model being the most rigorous. It should be noted that all of these analyses put forth theoretical models only and that dynamic calibration of the actual system must always be made before any pressure measurements are attempted.

Time-Averaged Pressure Measurement in an Unsteady Flow. The accurate evaluation of the time-averaged component of a fluctuating total pressure is essential in the design of turbomachinery. It is not

surprising then that many individuals have considered the measurement of the time-averaged component of an unsteady flow.

The system most often used to measure the time-averaged total pressure consists of a total pressure probe connected through a length of tubing to a slow-response pressure transducer. When this system is at equilibrium in a fluctuating stream, the pressure difference across the measurement holes is a function of the instantaneous mass flow rate through the holes. If this relationship is linear, then the indicated average pressure will be the same as the time-averaged pressure of the flow. However, if the relationship is nonlinear, which is the case with relations governing mass flow with respect to applied pressure, there can be a measurable difference between the indicated probe pressure and the actual time-averaged value. Samoilovich and Yoblov (15) have indicated in their work that the result of this may be either an underestimation or an overestimation of the level of losses in turbomachinery stages. Kronauer and Grant (16) propose that this error may be significant, as high as 15.0%, when the fluctuations are nonsymmetrical about the average. However, even though these large uncertainties exist, good approximations may still be made when working with small amplitude fluctuations. Krause, Dudzinski, and Johnson (17) have found this averaging error to be small, approximately 1.0% for small amplitude fluctuations.

Unsteady Flow Fluctuating Total Pressure Measurements. In measuring the instantaneous total pressure, the result of a large measuring volume between the pressure measuring hole and the transducer is a low resonant frequency of the system. The larger old-style transducer diaphragms made this large measuring volume necessary because

they could not be brought close to the flow without involving too large a resolution area or disturbing the local flow characteristics. As a result, probe frequency response was limited. Davis (18) and Strasberg (19) present pressure probes of this nature, both with low frequency response.

Siddon (20) developed a pressure probe and investigated the relationship between the time varying pressure amplitudes and probe resolution. The extent of the dependence of the pressure readings and turbulent eddy size were established; eddy size was of importance when the eddy scale was of the same order as or smaller than the probe's resolution dimension.

Armentrout (21) presented the applicability of miniature pressure transducers in the design of a high frequency response pressure sensing rake for use in turbofan engine tests. Since these transducers were highly sensitive to ambient temperature level change, a method of cooling to reduce this sensitivity was presented. Senoo, Kita, and Ookuma (22) used a modified cobra probe to measure instantaneous pressures at the exit of a pump impeller. The probe contained three semiconductor pressure transducers. Alarcon, Okiishi, and Junkhan (23) developed a fast-response total pressure probe for measurement of pressures in a low-speed multistage axial flow compressor. A miniature transducer was placed very close to the probe total pressure opening for fast response, and periodic-averaged total pressure measurements were made. The dynamic calibration of the probe was accomplished by subjecting the probe to a step change in total pressure and using the data obtained to form a second-order model.

In general, the fluctuating component (AC) can be measured with a good degree of precision with the help of miniature pressure transducers. This precision, however, is generally lost when measuring the time-averaged signal (DC) due to thermal zero shift. If temperature compensation is not provided, the AC and DC components are measured separately, with superposition of the two resulting in the absolute total pressure variation.

SCOPE OF THE INVESTIGATION

The objectives of this investigation are twofold: first, to design, construct, and calibrate a total pressure probe with a characteristically fast response time and, second, to use this probe to measure total pressure variations in an axial fan stage. The probe is intended to measure the complete total pressure variation (AC and DC). Zero shift error due to temperature fluctuation is avoided by using a temperature compensated transducer. As a comparison, a standard total pressure Kiel probe used with a slow-response transducer will also record the time-averaged pressure.

The probe design will utilize Bergh and Tjrdemar's (13) formulation for the prediction of the frequency response of the probe and phase shift. A computer program written by Nyland, Englund, and Anderson (14) will be used to facilitate this design.

Static calibration will be accomplished with the use of the Applied Research Laboratory's Open Jet Facility. Static sensitivity, as well as the probe sensitivity to Reynolds number and yaw and pitch angle, will be established. Dynamic calibration will be achieved through the construction of a sinusoidal pressure generating device known as a

Galton Whistle. With this whistle, the actual frequency response of the probe, as well as phase shift, can be measured.

Once static and dynamic calibration is complete, flow measurements will be taken in the Axial Flow Research Fan. Measurements will be taken downstream of the rotor at a fixed radial position for a uniform and a distorted rotor inflow.

CHAPTER II

PROBE DESIGN CONSIDERATIONS AND CONSTRUCTION

In conducting the design of a fast-response total pressure probe, one must consider a balance between aerodynamic, frequency response, and mechanical requirements. It is the optimization of these requirements that will provide the best design.

AERODYNAMIC REQUIREMENTS

The major aerodynamic concern in the design of total pressure probes for operation in subsonic flows is that of probe/flow misalignment. A simple impact tube with a square-edged opening will indicate a correct total pressure as long as the opening is aligned perpendicular to the flow. The accuracy of the measurement decreases as the angle of flow misalignment is increased. This problem can be alleviated somewhat by inclusion of an internal chamfer in the inlet of the tube (24). Flow angle variations of up to 20° from the average direction can be tolerated by a probe of this design. For angles greater than this, a shielded probe (Kiel probe) is required.

Another aerodynamic consideration is that of the sampling error incurred when probing a total pressure gradient, such as that caused by a viscous wake. Due to this gradient, the measured pressure does not represent the pressure that exists on the tube's centerline, but rather some spatially averaged value. This problem can be minimized by making the sampling tube diameter as small as possible.

Reynolds number effects will be noticeable only for a very slow moving fluid; stream blockage should be minimized by having a small frontal area and low drag coefficient. Interference from the probe support can be minimized by having the sensing hole at least three or more support diameters upstream of the support.

FREQUENCY RESPONSE REQUIREMENTS

If a second-order analysis is used to estimate the probe's response, one would want a resonant frequency as high as possible, in order that the probe would precisely measure the pressure variations. In the case of the use of a Galton Whistle, or a similar calibration device, the actual calibration curve is obtained, and the resonant frequency need only be as high as necessitated by the flow to be measured. However, an attempt should be made to have a flat response in the frequency range in question to facilitate ease of data reduction.

Pressure fluctuations due to turbulence would present a problem if periodic-averaged data were not taken. However, as explained in Chapter V on Probe Application, turbulent fluctuations are averaged out with this procedure (also known as ensemble averaging) and, therefore, need not be considered for the applications considered in this study.

MECHANICAL REQUIREMENTS

Because of the possibility of transducer failure, or should it be required to be removed for any other reason, the probe should be designed with ease of its removal in mind. This means more permanent methods, such as cementing in place with a sealant, cannot be employed.

Probe strength and stiffness should be taken into account when measuring unsteady flows, such as those present in turbomachinery. Any

vibration of the probe would contribute to inaccuracies in the resulting measurements. The ease of manufacturing is another point not to be overlooked. A well-designed probe is one that is as simple and economic to construct as it is accurate and reliable to use.

Finally, the probe should be of a configuration that is easily mounted. A round tubular shape would seem to be the best for most turbo-machinery applications.

PROBE DESIGN AND CONSTRUCTION

Probe. The probe considered in this study was designed with the general guidelines discussed above in mind. As shown in Figure 2, the transducer is located inside the probe body, with a modified United Sensor 1/8-inch Kiel probe positioned to form a mounting cavity. This provides excellent probe head characteristics, making it relatively insensitive to flow misalignment and support interference. (This will be established during static calibration of the probe.) The reference pressure of the transducer is atmospheric, vented by way of the support body.

As mentioned earlier, theoretical predictions of the probe frequency response and phase shift were made using Bergh and Tijdeman's (13) formulation, in the form of Nyland, Englund, and Anderson's (14) computer program. This program was rewritten to be acceptable to the Applied Research Laboratory's IBM 1130 computer and restricted to the calculation of one tube/cavity system. Bergh and Tijdeman's formulation for a single tube/cavity system is included in Appendix A, along with predictive frequency response data obtained from the rewritten computer program.

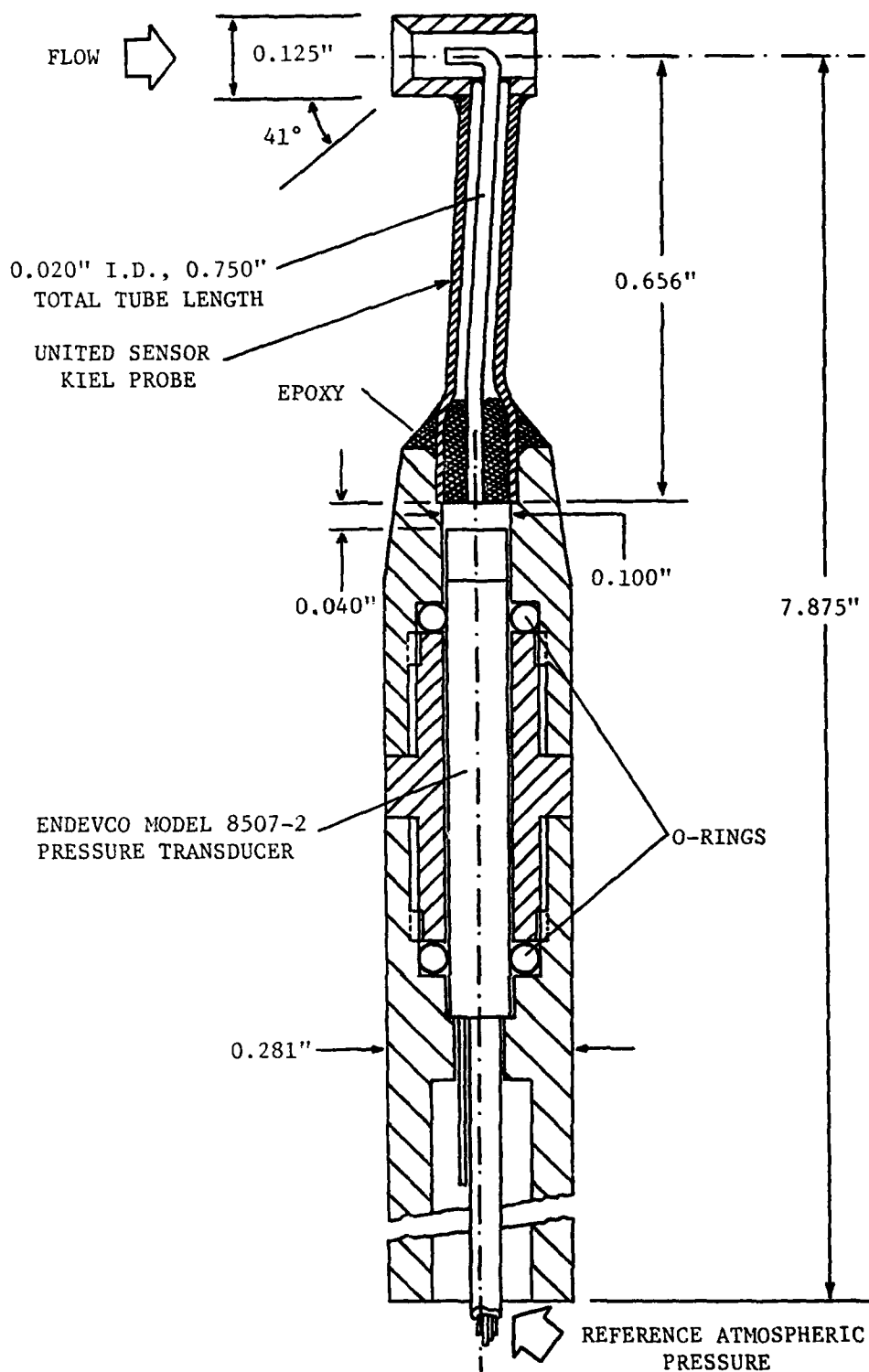
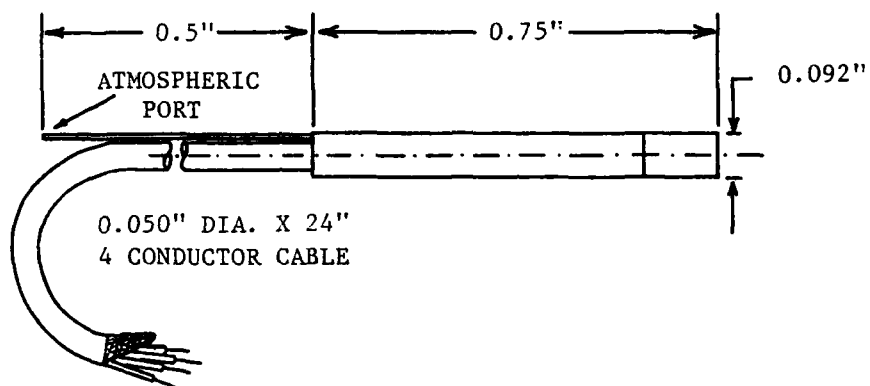


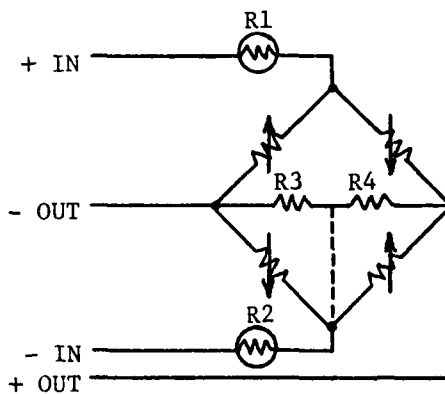
FIGURE 2. FAST-RESPONSE KIEL PROBE

Pressure Transducer. The pressure transducer, an Endevco Model 8507-2, is shown in Figure 3. The sensor design is an active four-arm piezo-resistive Wheatstone bridge, diffused directly onto a shaped silicon chip. It incorporates integral temperature compensation through the range of 50 to 150° Fahrenheit. This circuitry is completely housed within its small cylindrical base. Transducer specifications are given in Table 1.

An examination of the predicted probe response indicates that resonance will occur at approximately 1,530 Hz. The main factor contributing to this value was the choice of the United Sensor Kiel probe as the fast-response probe's head. This mechanical constraint was imposed to provide a greater ease of construction and good insensitivity to flow direction. Much higher resonant frequencies can easily be obtained by relaxing this constraint through the selection of the tube/cavity configuration.



(a)



R1 & R2:
THERMAL SENSITIVITY
SHIFT ADJUSTMENT

R3 & R4:
ZERO BALANCE ADJUSTMENT

(b)

FIGURE 3. PRESSURE TRANSDUCER: (a) TRANSDUCER DETAIL, (b) BRIDGE CIRCUITRY

Table 1
 Transducer Specifications*

Range:	2 psig
Resonant Frequency:	45,000 Hz
Sensitivity:	157 ±45 mv/psi
Zero Shift Across Temperature Range:	±3.0% of Full Scale Output
Maximum Sensitivity Shift Across Temperature Range:	±3.0% of Full Scale Output
Temperature Range:	50 to 150 ^o Fahrenheit
Burst Pressure	
Minimum Differential:	±40 psi
Maximum Case:	50 psi
Excitation	
Rated:	10 V DC
Maximum:	18 V DC
Resistance	
Input:	1,800 ohms
Output:	1,600 ohms
Isolation:	>20,000 megohms at 50 V
Acceleration Sensitivity	
Longitudinal:	0.0005 psi/g
Lateral:	0.0003 psi/g

* at rated excitation of 10 V DC

CHAPTER III

PROBE TESTING

This chapter presents a description of the static and dynamic tests used to calibrate the fast-response Kiel probe and the standard Kiel probe discussed in Chapter II. These tests were undertaken to determine the probe's aerodynamic and frequency response characteristics. The static tests deal with the influence of yaw and pitch angle and Reynolds number on the steady total pressure measured by the probe and the determination of its static sensitivity. Dynamic tests determined the probe's response to an unsteady pressure. Since the standard Kiel probe will only undergo an aerodynamic static calibration, the procedure for its calibration is identical to a portion of the procedure for the calibration of the fast-response Kiel probe. The results of this static calibration are included in the following discussion.

STATIC TESTS

The tests described in this section were all carried out using the Applied Research Laboratory's Open Jet Facility, pictured in Figure 4. This facility has a throat diameter of 12 inches and a contraction ratio of 30 to 1, with a maximum tunnel throat velocity of 115 fps. For calibration purposes, the probe was positioned one throat diameter from the nozzle exit and, at all times, remained well in the core flow. Figure 5 is a close-up of the probe holding device. Pressure differentials were obtained using a Validyne variable reluctance

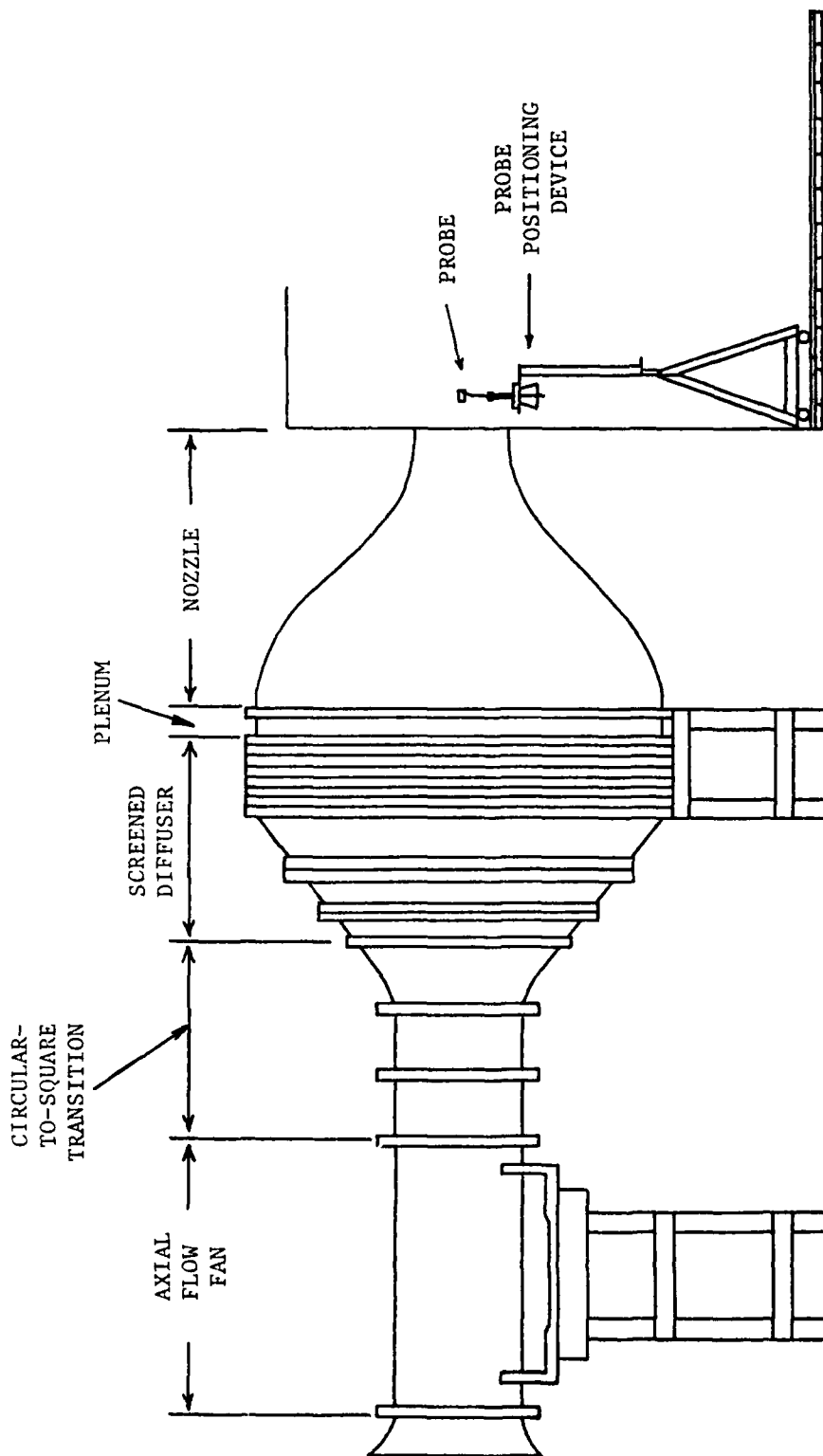


FIGURE 4. OPEN JET FACILITY

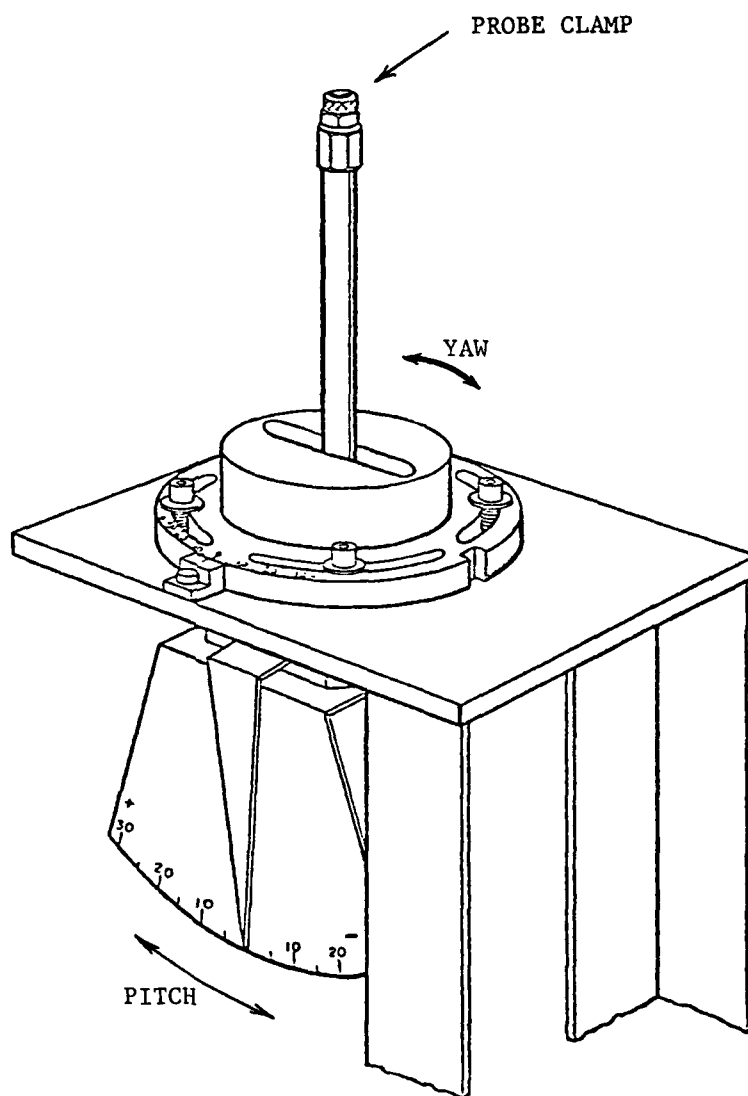


FIGURE 5. PROBE HOLDING DEVICE SHOWING YAW/PITCH MECHANISM

transducer. (A calibration plot for this transducer (T-1) may be found in Appendix B.) A schematic of the entire test setup is shown in Figure 6.

Reynolds Number and Yaw and Pitch Angle Calibration. To determine the effect of Reynolds number, the probe, without its transducer installed, was aligned with the flow: yaw and pitch angles as defined in Figure 7 were identically zero. The pressure difference between the Open Jet's plenum pressure, P_p , and the probe indicated total pressure, P_T , was then examined over the flow velocity range expected in the Axial Flow Research Fan. The results are given in Figure 8. The standard Kiel probe showed negligible influence of velocity level on indicated total pressure. The fast-response Kiel probe showed a relatively small, constant loss of approximately 1.5%.

The effect of flow angle was examined next. At velocities of 40, 65, and 90 fps, the probe yaw angle was varied $\pm 35^\circ$ with the pitch angle equal to zero. Next, the probe pitch angle was varied $\pm 30^\circ$ with the yaw angle equal to zero. The pressure difference between P_p and P_T was examined through both these ranges and the results are given in Figure 9. The standard Kiel probe showed negligible influence of yaw and pitch angle over the entire range tested. The fast-response Kiel probe again showed a loss of approximately 1.5% over the entire range.

The constant 1.5% loss indicated in the fast-response Kiel probe tests was suspicious, especially since the data were obtained six months after the standard Kiel probe tests. A clogging of the flow straightening screens in the open jet was suspected, as this would cause increased losses due to the higher level of turbulence. The standard Kiel probe Reynolds number test was rerun, and the results (given in

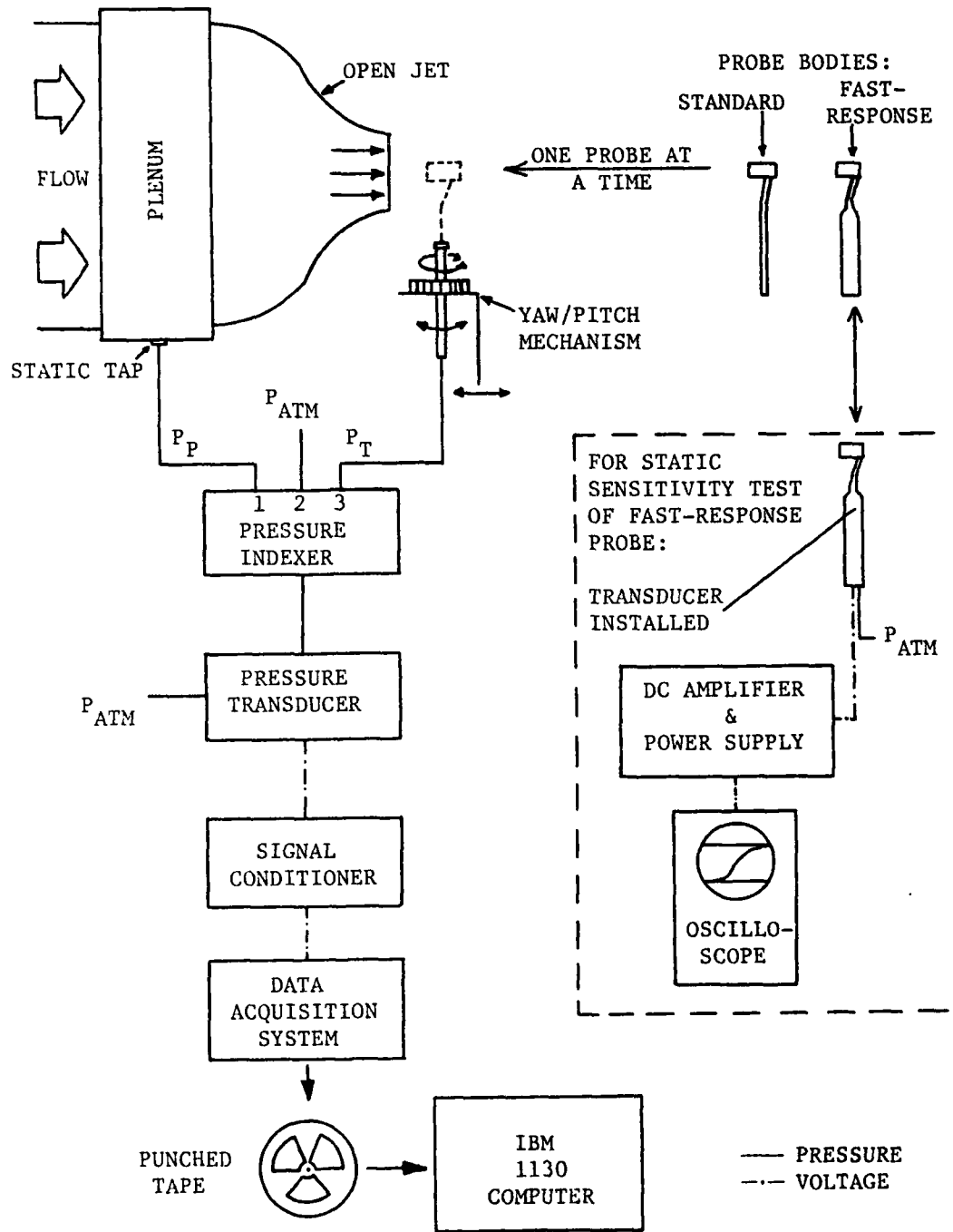


FIGURE 6. SCHEMATIC OF THE STATIC TEST SETUP

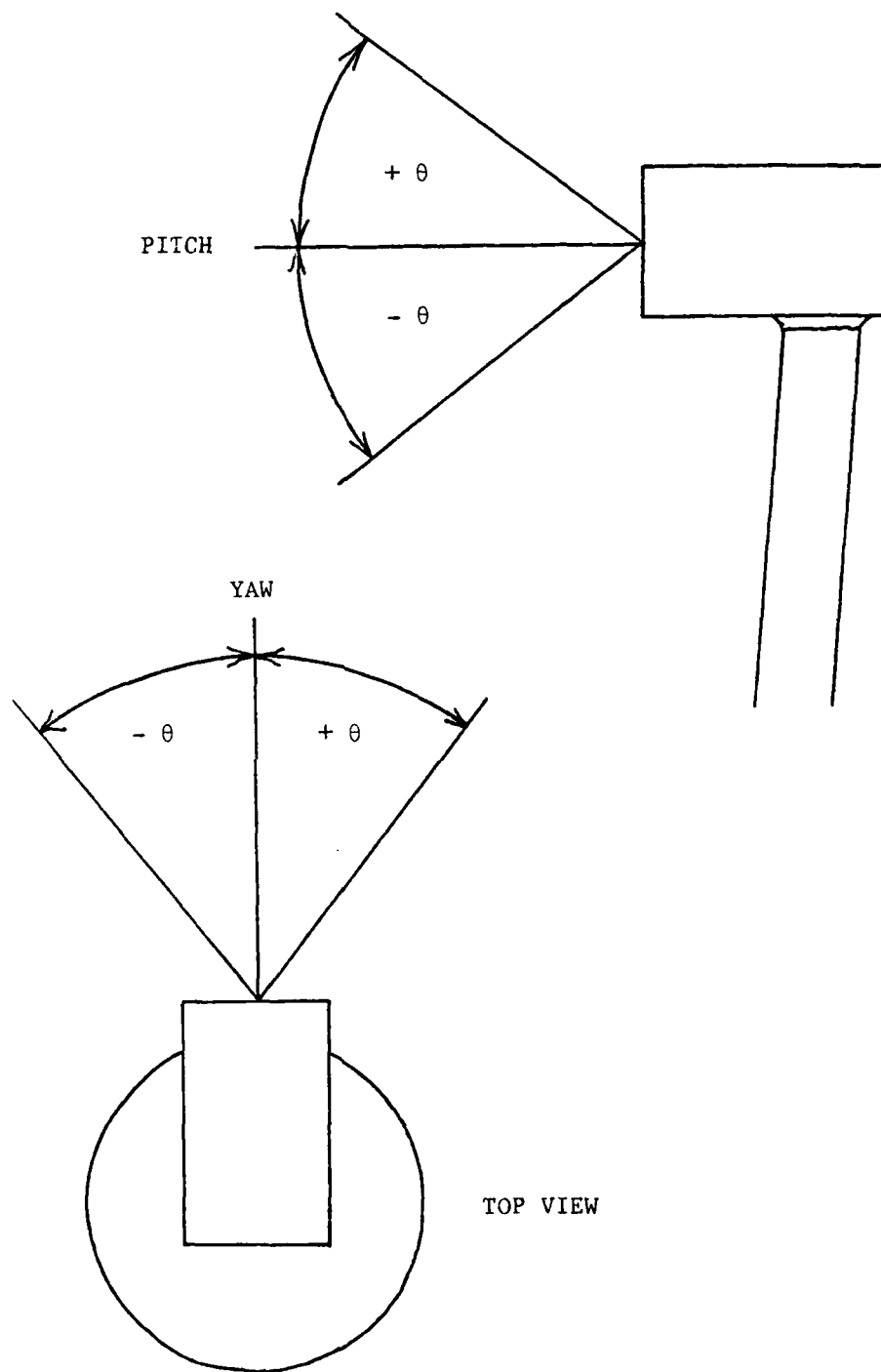


FIGURE 7. YAW/PITCH ANGLE DEFINITION

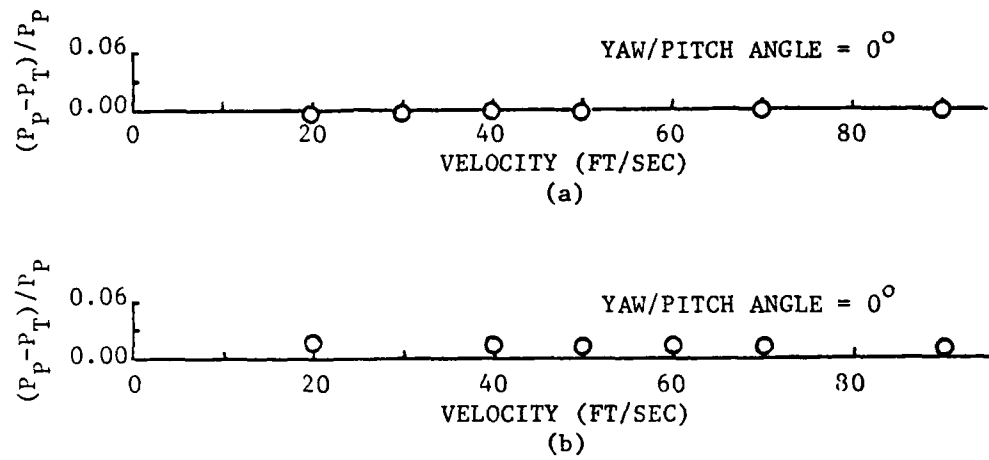


FIGURE 8. REYNOLDS NUMBER CALIBRATION CURVES: (a) STANDARD KIEL PROBE, (b) FAST-RESPONSE KIEL PROBE

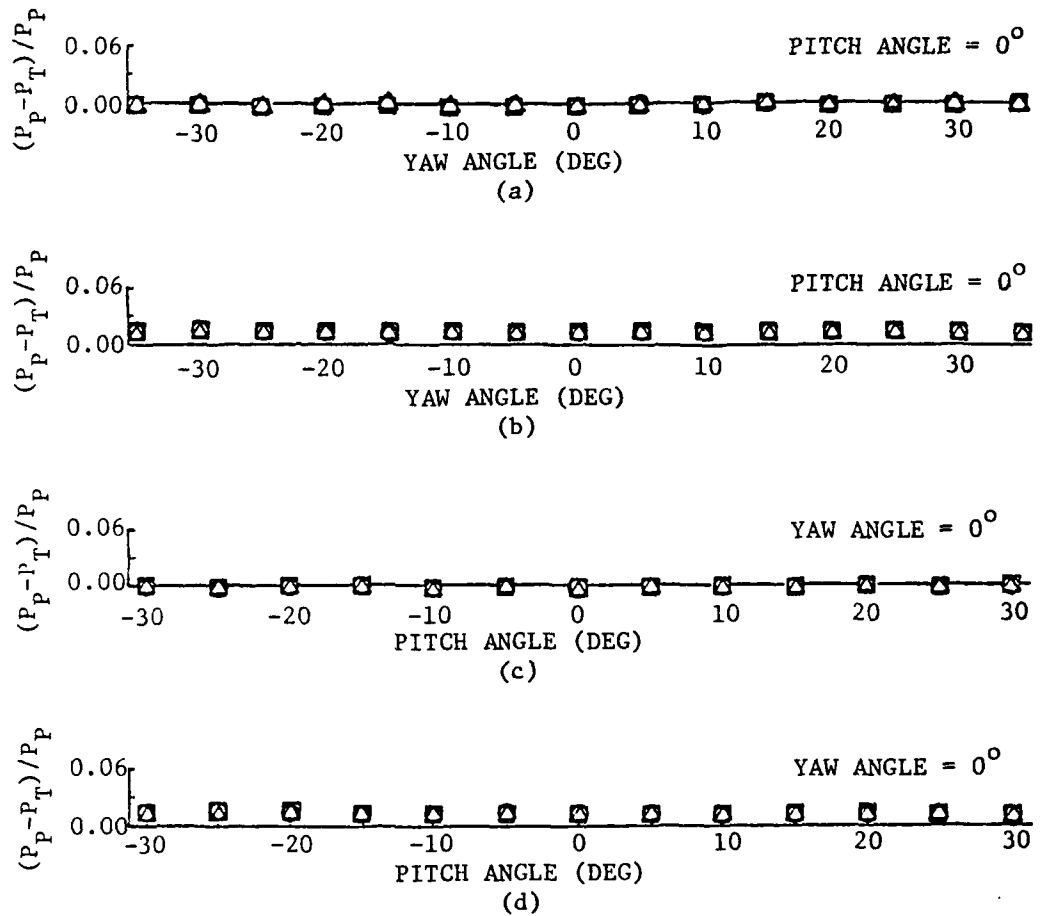


FIGURE 9. YAW/PITCH ANGLE CALIBRATION CURVES: (a) AND (c) STANDARD KIEL PROBE, (b) AND (d) FAST-RESPONSE KIEL PROBE

Appendix B) indicate that there was now a significant loss associated with the Open Jet of approximately 2.0%. Thus, the fast-response Kiel probe has a very small loss, less than 0.5%.

Static Sensitivity Calibration. The transducer was then installed in the fast-response Kiel probe to determine its static sensitivity. The probe was aligned with the flow, and plenum/probe differential pressure was examined. Initial test results indicated a significant zero shift when the probe was immersed in the flow, making an accurate determination of probe sensitivity difficult. Since direct contact of the transducer and probe body occurs at the base of the transducer, it is possible that mechanical stresses are being impressed on the transducer by expansion/contraction of the probe body.

As an immediate solution to this problem, the following method used by Alarcon, Okiishi, and Junkhan (23) was employed. The output of the probe was displayed on a storage oscilloscope, and the signal was zeroed. The probe was then exposed to the flow, and the rise in pressure read off the scope, which had been previously calibrated. The results of this method are shown in Figure 10. The method to overcome this zero shift during data acquisition in the AFRF will be discussed later.

DYNAMIC TESTS

Whenever a fast-response probe is designed, its theoretical dynamic response must be checked by actual calibration of the probe. The calibration device chosen was a sinusoidal pressure generator based on the Galton Tube. It consists of a resonant tube driven by an annular air jet, impinging on its knife edge. The design of this "whistle" was modeled after one presented by Nyland, Englund, and Gebben (25). It is

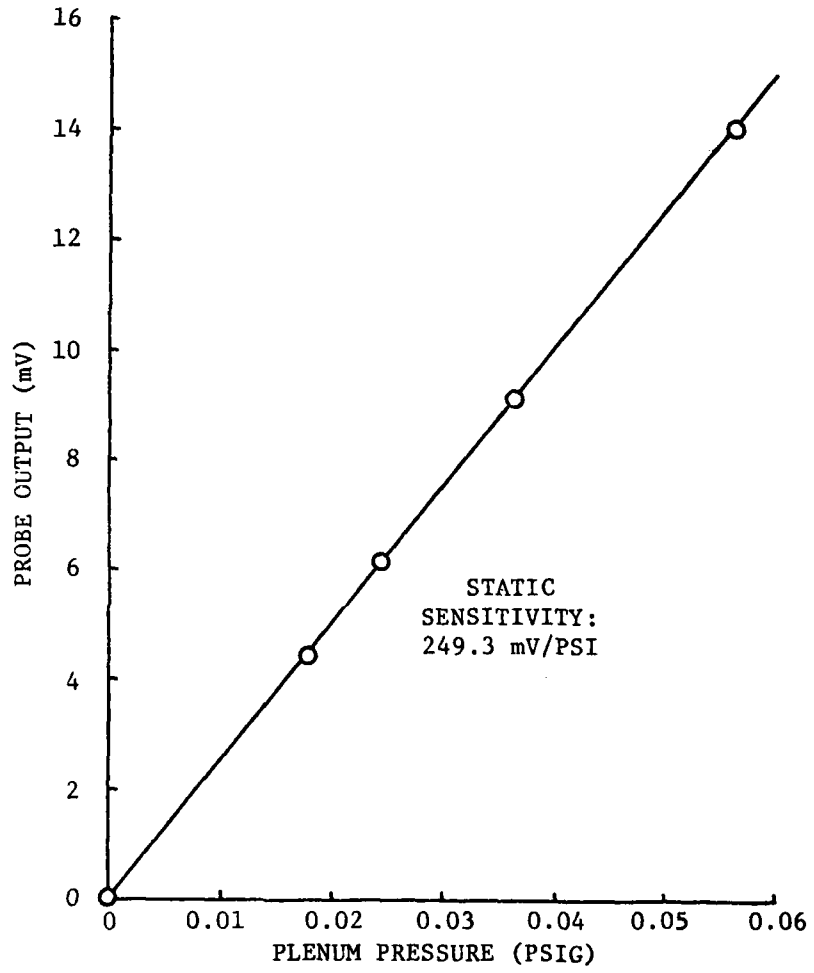


FIGURE 10. FAST-RESPONSE KIEL PROBE STATIC SENSITIVITY CALIBRATION CURVE

capable of generating relatively clean sinusoidal waves in the 250 to 2,200 Hz range with peak-to-peak amplitudes of 0.8 psi.

A drawing of the basic generator is shown in Figure 11. The resonant tube is constructed of 0.065-inch wall, 1-inch diameter tube. The open end of the tube is tapered at an angle of 30° with respect to the tube axis to form a sharp edge at the inside tube diameter. The nozzle consists of an annular opening 0.03 inch in width, aligned with this knife edge. Pressure ports are located along the length of the tube. At each axial position, there are four circumferentially positioned ports: one for a reference transducer, one for the transducer to be tested, and two spares.

The whistle operates as follows. Air flowing through the nozzle impinges on the tapered edge of the tube. The resulting turbulence induces the air in the tube to oscillate, setting up a standing wave. The pressure generated at any point along the length of the resonator is given by the approximation

$$p = P \sin \left(\frac{\pi}{2} \frac{n}{L} X \right) \sin (2\pi ft) \quad , \quad (1)$$

with

$$f = \frac{nc}{4L} \quad (2)$$

and

p = pressure at any point along the resonator,

P = peak pressure amplitude,

L = resonator length,

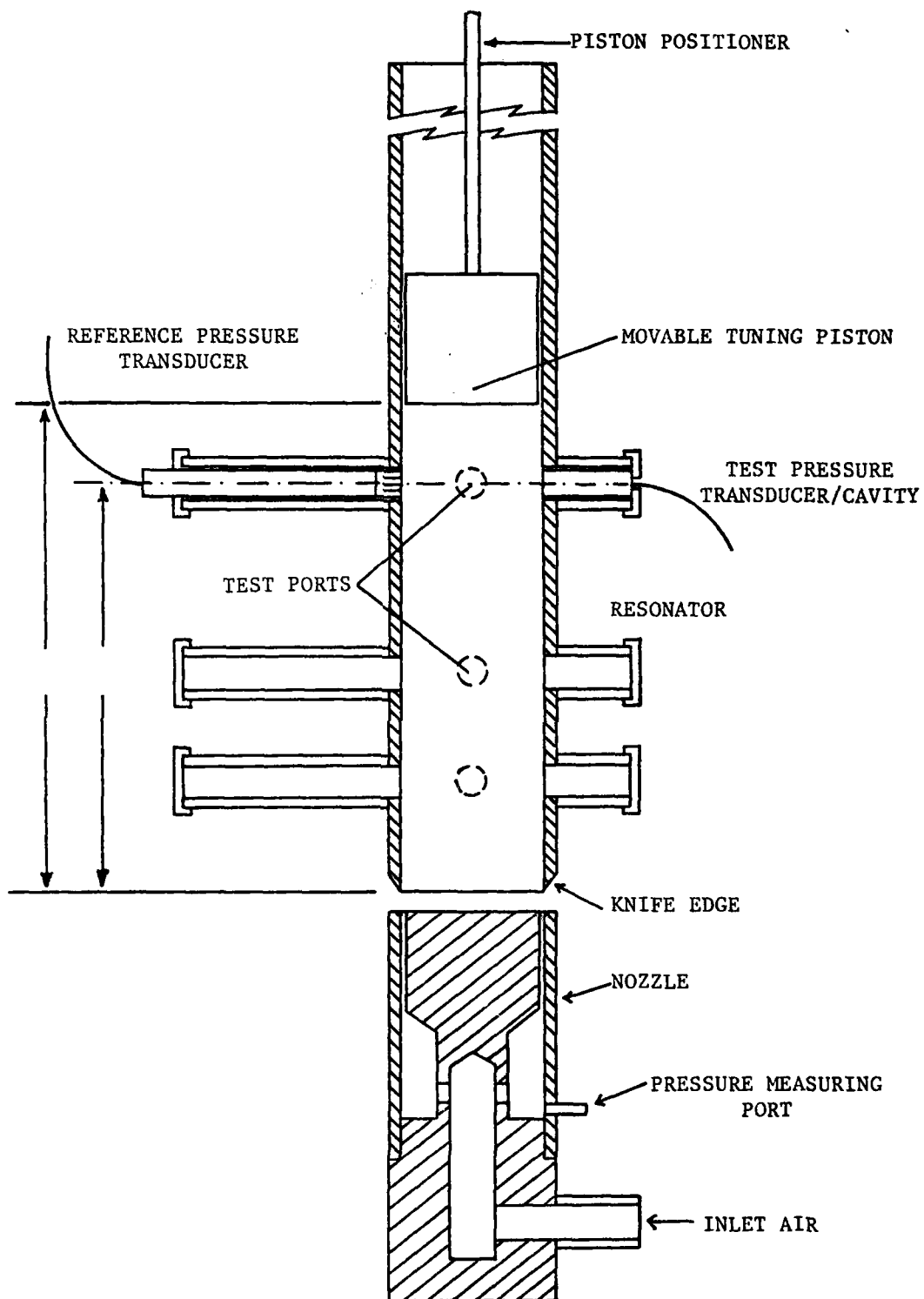


FIGURE 11. BASIC GALTON WHISTLE CONFIGURATION

X = distance from knife edge to center of port,

f = frequency of oscillation,

t = time,

c = local speed of sound, and

n = mode number (1, 3, 5, ...).

The resonator can oscillate in many different modes, depending on the pressure drop across the nozzle and nozzle-to-resonator spacing. The peak pressure amplitude, P , is mainly a function of pressure drop across the nozzle, but it will also vary with nozzle-to-resonator spacing. Once oscillating in a mode, the frequency of the oscillation is only a function of tube length, assuming a constant local speed of sound. The ports have been spaced so that, for any given oscillation, a set of ports will be available where the pressure amplitude is within 75.0% of the maximum or peak value. Thus, by varying the length of the tube, the nozzle-to-resonator spacing, the pressure drop across the nozzle, and the choice of ports, one can obtain a spectrum of frequencies and amplitudes.

To obtain an idea of the operating characteristics of the whistle, a plot of peak-to-peak pressure amplitude versus pressure drop across the nozzle was first obtained. The pressure drop across the nozzle was measured with a slant tube manometer, while peak-to-peak pressure amplitudes inside the resonator were measured with a flush mounted 1/4-inch Brüel and Kjaer microphone. This microphone has a flat response in the 200 to 9,000 Hz range. All points were obtained by adjusting the pressure drop and nozzle-to-resonator spacing to get a sinusoidal wave operating in one mode with minimum waveform distortion, as shown by an oscilloscope trace. This plot is given in Figure 12.

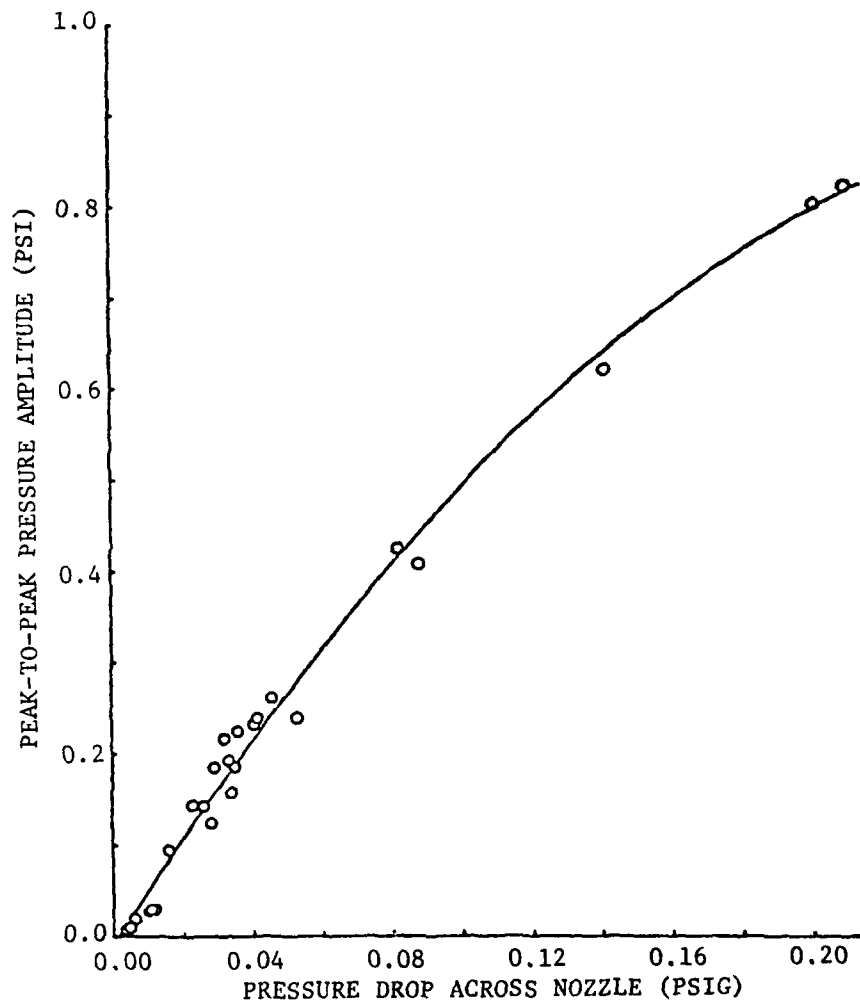


FIGURE 12. GALTON WHISTLE RESPONSE CURVE

Probe Calibration. To dynamically calibrate the fast-response Kiel probe, the setup in Figures 13 and 14 was used. Since the probe itself could not be mounted in the resonator tube, a simulation of the probe cavity/transducer arrangement was constructed. The simulator duplicates the internal flow passages of the probe itself, as well as the manner in which the transducer is mounted in the probe, and can readily be mounted in the whistle. The only difference is the bend in the head of the actual probe; exclusion of this bend will not affect the probe's characteristics as long as its diameter is constant and its radius is of the same order of magnitude as the tubing length (11). The simulator is pictured in Figure 15.

For all calibration data, the simulator was mounted directly opposite the reference transducer, a 1/4-inch Brüel and Kjaer microphone, used in conjunction with a Model 2603 Brüel and Kjaer microphone amplifier. The test transducer output was routed through a Danna Model 3520 DC amplifier and inputted into the Brüel and Kjaer amplifier, which was calibrated to read in peak volts. In addition, the output of both transducers was channeled into a Spectral Dynamics Model SD110 phase meter, and a frequency counter was connected to the reference transducer.

To calibrate the simulator, the test transducer was excited by a constant 15 V DC source (± 0.01 V DC); amplitude gain and phase lag as a function of the frequency of oscillation were recorded. The results are plotted in Figure 16, along with predicted response curves obtained using Bergh and Tijdeman's formulas (13). (To insure repeatability, a second test run was taken; both are included in Appendix A.) Test data indicated resonance occurs at approximately 1,500 Hz, as compared to 1,530 Hz predicted.

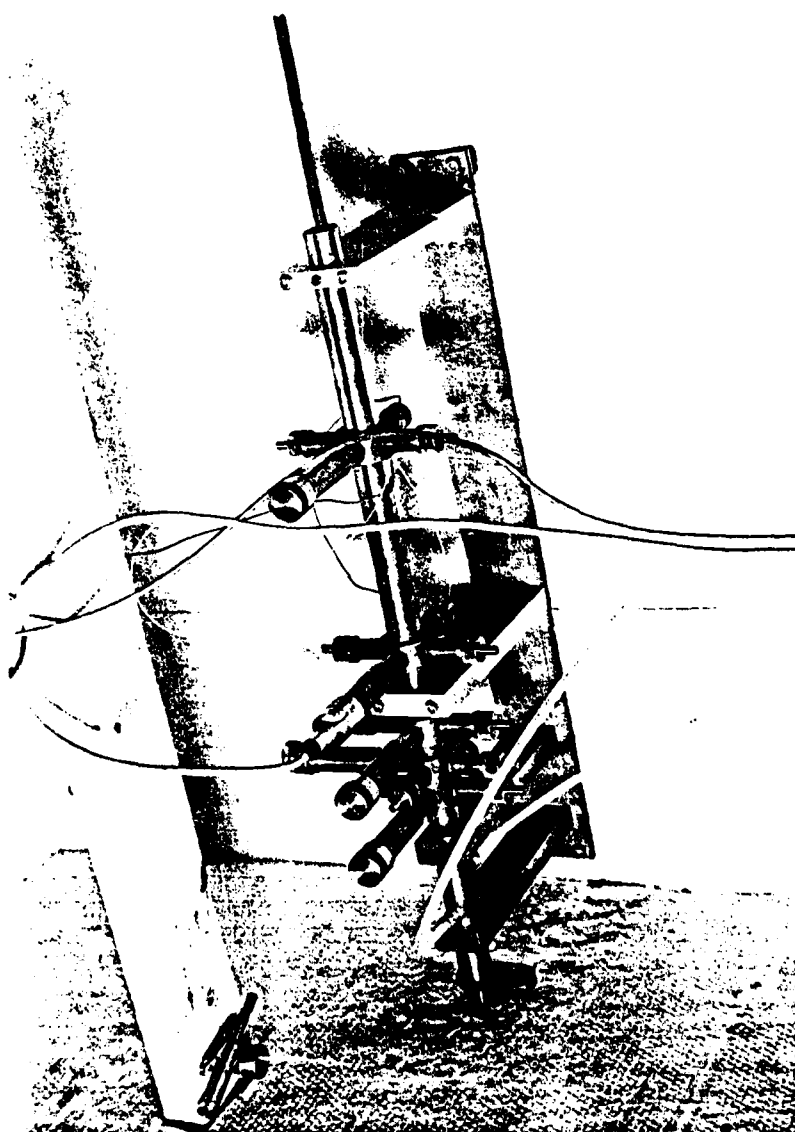


FIGURE 13. GALTON WHISTLE, SHOWING THE FAST-RESPONSE KIEL PROBE'S SIMULATOR AND THE REFERENCE TRANSDUCER MOUNTED AT A TYPICAL LOCATION

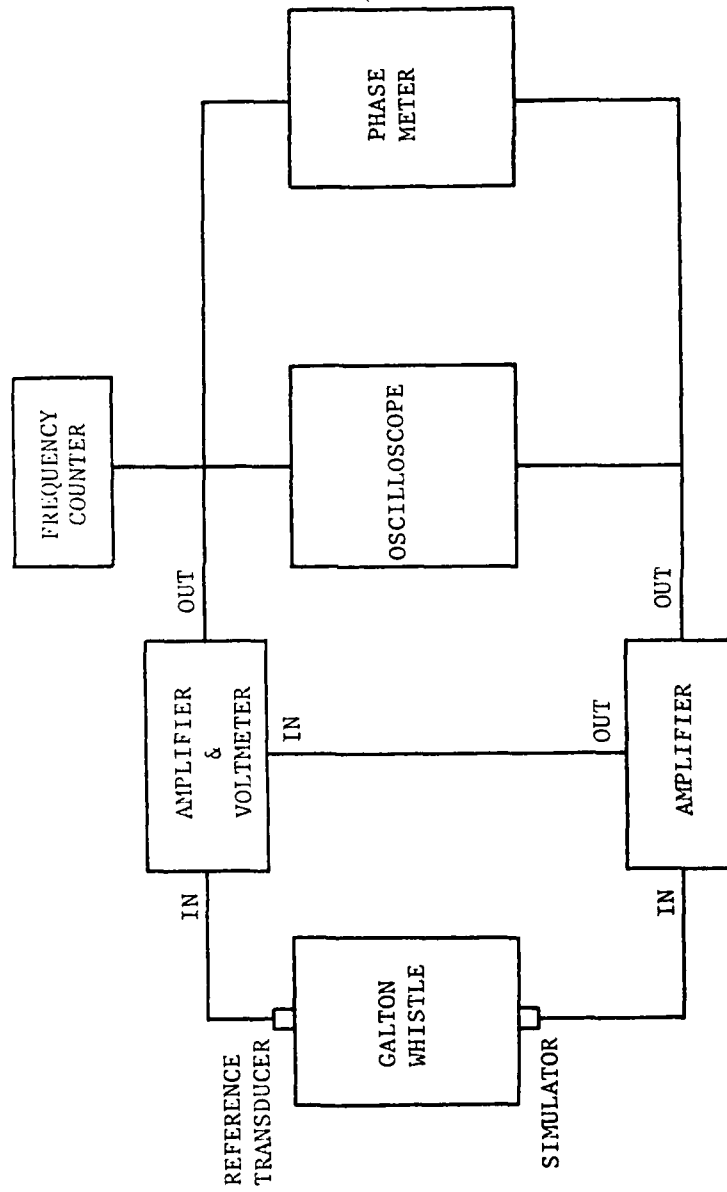


FIGURE 14. SCHEMATIC OF THE DYNAMIC CALIBRATION SETUP

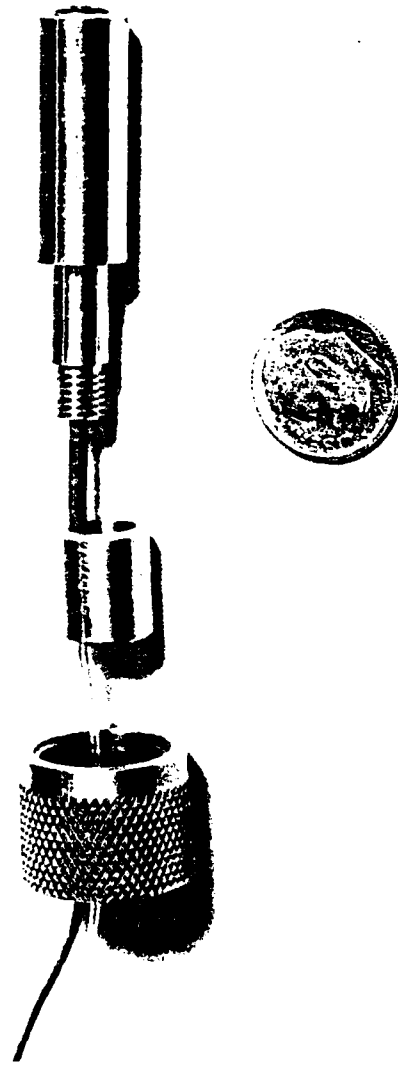


FIGURE 15. CLOSE-UP OF THE FAST-RESPONSE KIEL PROBE'S SIMULATOR

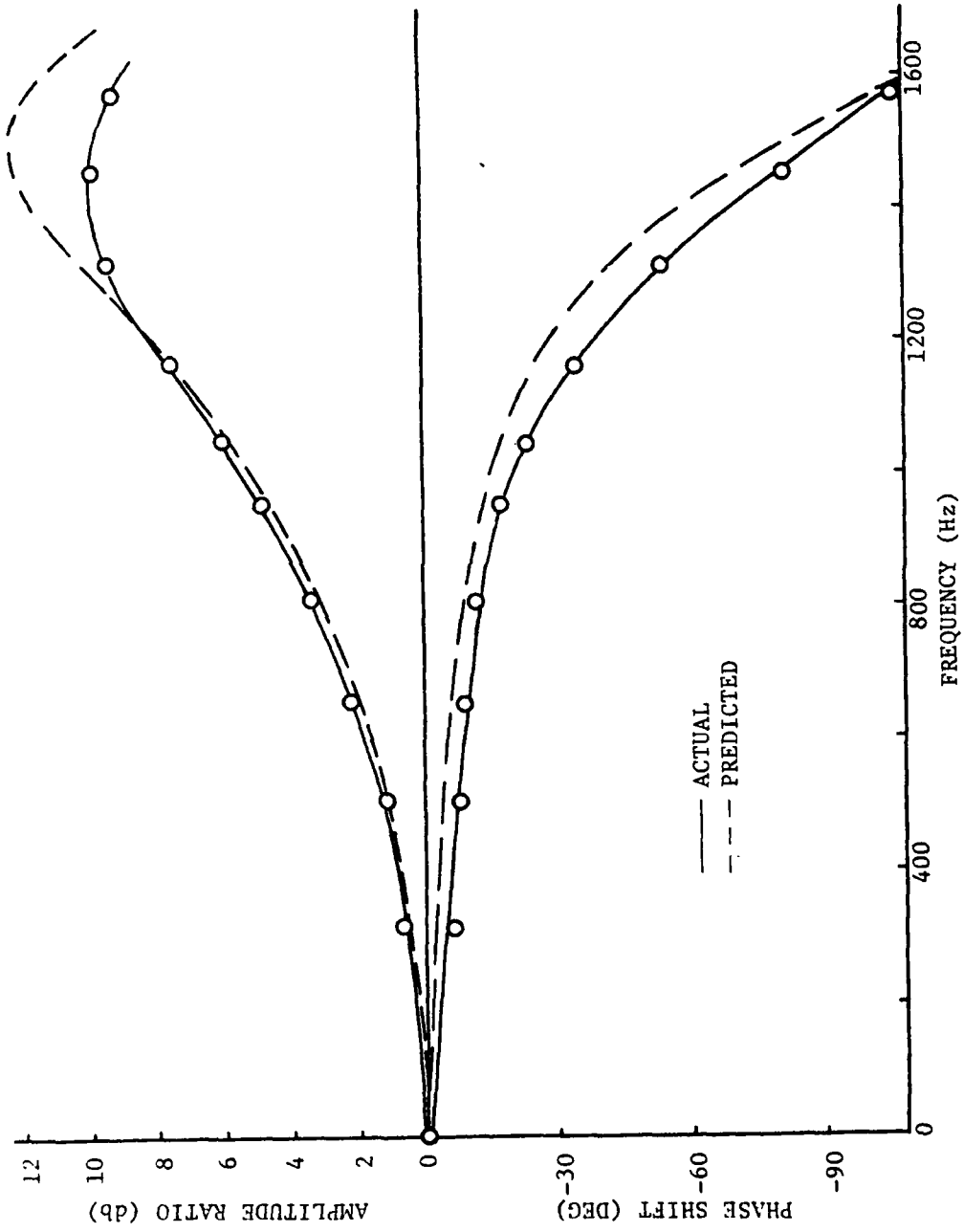


FIGURE 16. FREQUENCY RESPONSE CURVES OF THE FAST-RESPONSE KIEL PROBE'S SIMULATOR

CHAPTER IV

RESEARCH FACILITY

AXIAL FLOW RESEARCH FAN

The Axial Flow Research Fan (AFRF) of the Applied Research Laboratory at The Pennsylvania State University, Figure 17, was used in the present study. The 19-2/3-foot fan consists of a bellmouth inlet leading into an annular flow passage containing a rotor and auxiliary fan and ending in an exhaust throttle. The entire forward section, from inlet to just upstream of the rotor drive motor, is bounded by a 21-1/2-inch inside diameter casing and a 9-1/2-inch diameter hub surface.

The rotor, composed of nine circular arc cambered blades, includes one blade instrumented to measure unsteady lift and moment. These aluminum blades have a maximum thickness-to-chord ratio of 10.0% and were designed as part of a free vortex loaded stage that includes an eight-bladed stator. This stator, however, was removed for these tests. The rotor is driven by a 70 Hp motor located in the center hub, downstream of the test section.

The auxiliary fan delivers 15,000 cubic feet of air per minute at a pressure of 3.5 inches of water gauge at its nominal operating condition. The auxiliary fan drive motor and the 70 Hp motor are independently regulated through the use of two solid state adjustable frequency drive inverter units.

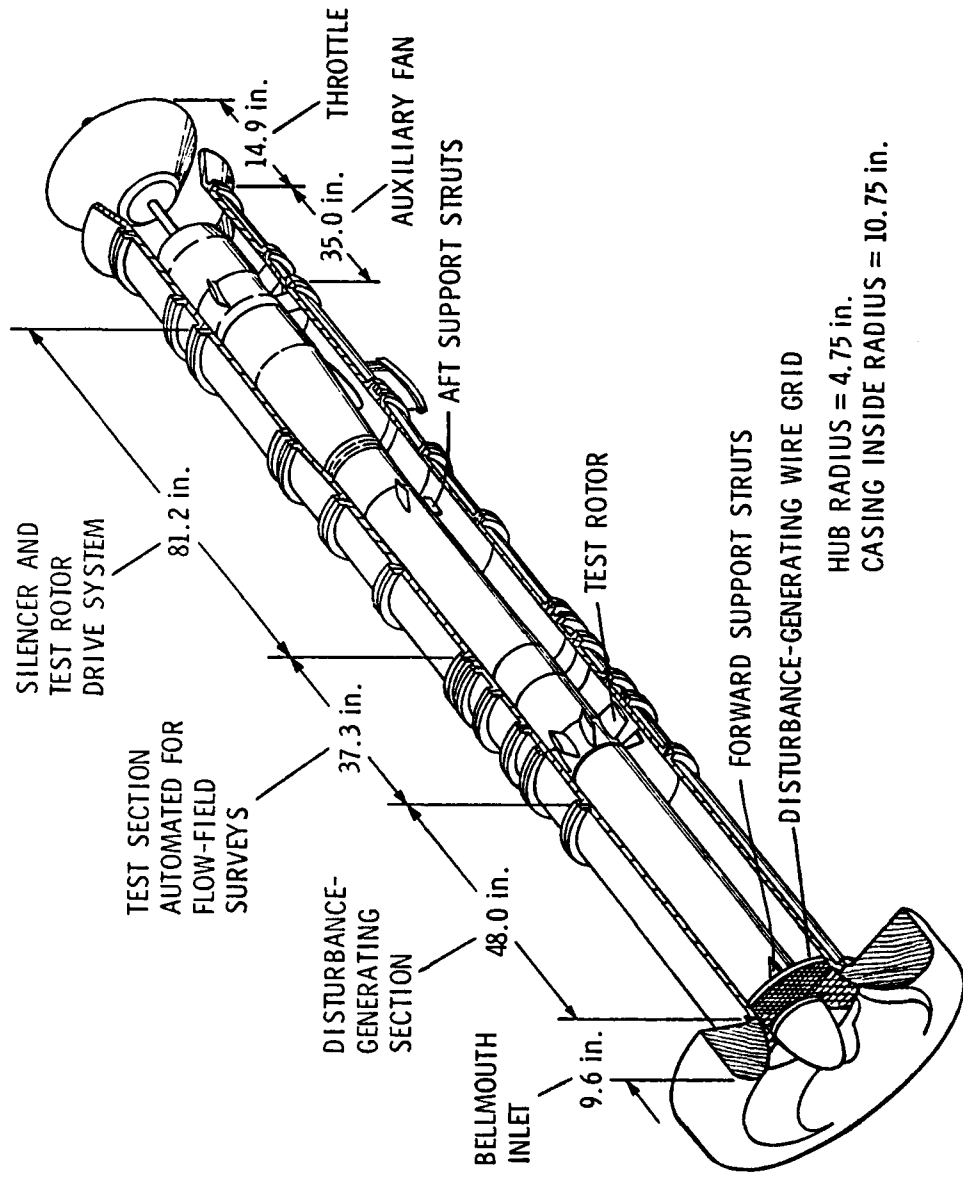


FIGURE 17. AXIAL FLOW RESEARCH FAN

A foam and screen-covered wooden housing projects upstream of the bellmouth opening. It was installed there to remove any turbulence or rotation that may exist in the inlet flow.

The 48-inch section just downstream of the bellmouth inlet houses a disturbance generating section. Honeycomb, wire grid, or cylindrical rod obstructions may be placed in the flow to develop many distorted inflow configurations (1, 3).

The rotor, housed in the next downstream section, is surrounded by an other casing that can be rotated about the AFRF centerline. This feature permits circumferential surveying of the flow with casing mounted probes.

For a more detailed description of this test facility and its present capabilities, see References (1) and (26).

FLOW MEASURING INSTRUMENTATION

A schematic drawing is shown in Figure 18 of the instrumentation used to measure the flow field in the AFRF. This instrumentation system consists of two major sections, one to determine the instantaneous total pressure and the other to determine the time-mean flow. The entire instrumentation arrangement is composed of:

- (1) fast-response total pressure Kiel probe,
- (2) DC amplifier and power supply (Danna Model 3520),
- (3) photoelectric triggering circuit,
- (4) digital signal processor (Spectral Dynamics Model SD360),
- (5) tracking ratio tuner (Spectral Dynamics Model SD134A),
- (6) X-Y display (Spectral Dynamics Model SD311),
- (7) X-Y plotter (Hewlett-Packard Model 7010A),

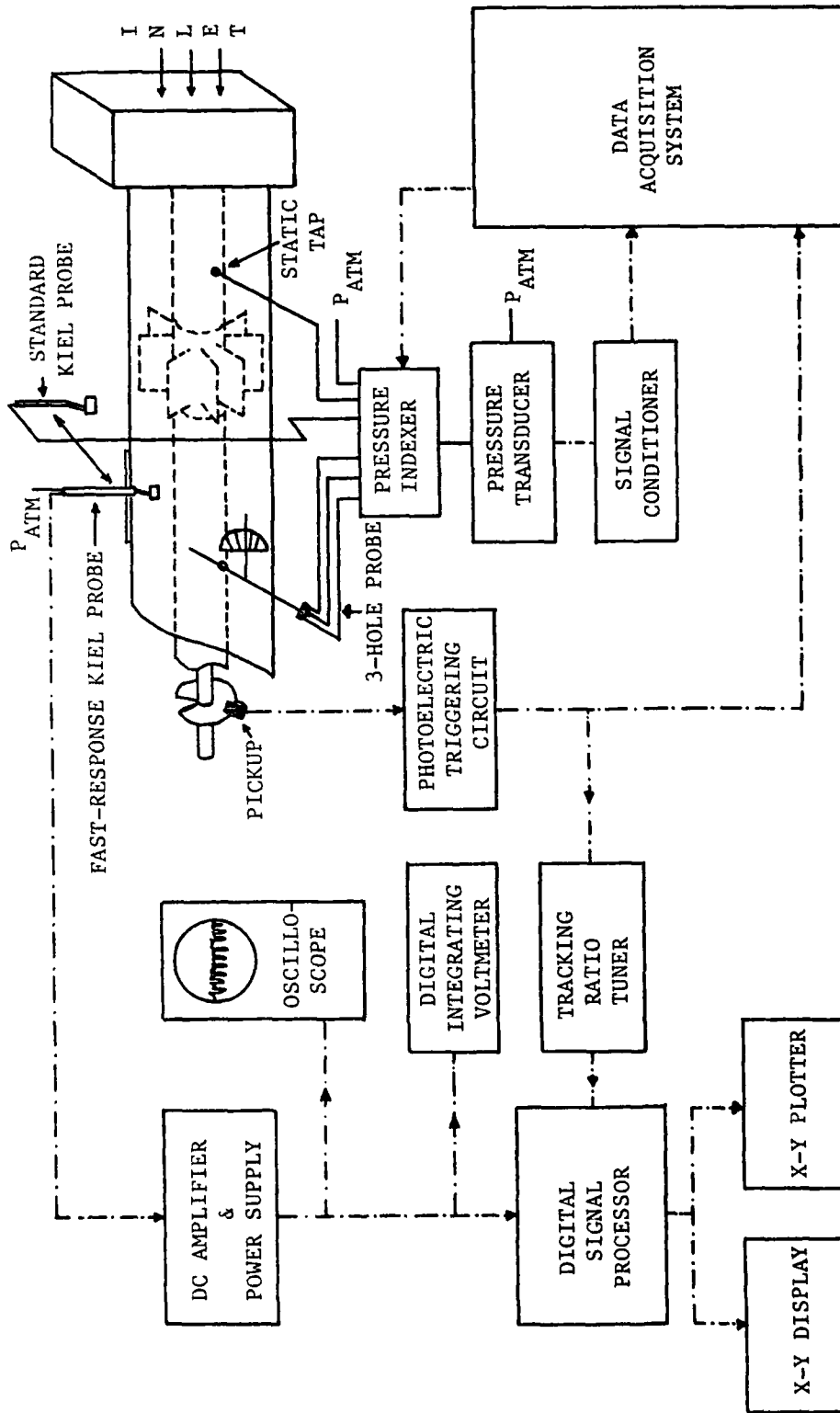


FIGURE 18. SCHEMATIC OF THE FLOW MEASUREMENT INSTRUMENTATION

- (8) digital integrating voltmeter (Dymec Model 2401C),
- (9) oscilloscope (Tektronics Model 7603),
- (10) Kiel probe (United Sensor 1/8-inch),
- (11) variable reluctance pressure transducer (Validyne Model DP15),
- (12) signal conditioner (Validyne Model CD15),
- (13) data acquisition system,
- (14) three-hole wedge probe,
- (15) pressure indexer,
- (16) static pressure tap, and
- (17) probe positioners.

The digital signal processor is used in conjunction with the photoelectric triggering circuit and the tracking ratio tuner to analyze the output of the fast-response total pressure probe. When operating in the time domain, this processor (Spectral Dynamics SD360) is able to ensemble average the input signal. This consists of the pointwise averaging of the signal over consecutive rotor periods. Signals periodic with the rotor period will be preserved, while random signals and those which are nonperiodic with respect to the rotor revolution will diminish as the number of periods averaged is increased. The photoelectric triggering circuit provides a once per revolution pulse used to synchronize the phase of each rotor period. This synchronization is achieved by the tracking ratio tuner, which interfaces the triggering circuit and the digital signal processor. The result is a digitized periodic-averaged total pressure signal. Additional circuitry within the processor provides for operation in the frequency domain, as well as a Fast Fourier Transform capability.

The time-mean data acquisition system was designed and built at the Applied Research Laboratory, The Pennsylvania State University. It controls the channel selection of the pressure indexer and time averages input signals over a one-second interval. In addition, it records each voltage, as well as rotor rpm, on punched tape.

The three-hole wedge probe was used in conjunction with the probe positioners to align the standard and fast-response total pressure probes with the flow. The three-hole probe indicates flow angle by rotating the probe until both static taps are equalized and then reading a protractor scale attached to the casing. Similar scales on each total pressure probe allow them to be aligned with the flow. In its downstream position, the three-hole probe will not accurately measure the flow angle that exists at the rotor exit due to the flow gradients caused by the rotor wakes. However, tests have shown the measurements to be within $\pm 5^\circ$. Since the exact probe angle is not critical due to the demonstrated insensitivity of the Kiel probe to changes in flow angle, Figure 9, this method will suffice.

A static tap, located 42 inches downstream of the bellmouth exit was used to determine the inlet axial velocity at the mean radius. For uniform inflow, the following relation was used:

$$V_{AVG} = \sqrt{\frac{2(P_{ATM} - P_S)}{\rho}} \quad (3)$$

The quantity $(P_{ATM} - P_S)$ is the differential pressure measured at the static tap, and ρ is the density of air calculated from the ideal gas equation. For a distorted inflow, the average axial inlet velocity at the mean radius was obtained using previously measured test data which

relate the static casing pressure at this location and the circumferentially mean axial velocity (27). A plot of this relationship is included in Appendix B for the distorted inflow described in the next chapter.

CHAPTER V

PROBE APPLICATION

Previous aerodynamic testing has demonstrated the fast-response Kiel probe to be relatively insensitive to flow direction and Reynolds number in the range examined. The tests presented in this section are meant to give an indication of the applicability of a probe of this type to flows found in turbomachinery and to compare these measurements to those of the time-mean total pressure obtained with a standard Kiel probe.

DATA ACQUISITION

The fast-response Kiel probe was subjected to the three test conditions listed in Table 2. The first two tests were run with a uniform inflow velocity to the rotor, while, in the last test, a four-cycle velocity distortion was created with the use of a screen placed in the inlet. This screen is shown in Figure 19.

In each test, the fast-response Kiel probe's signal was ensemble averaged over 1,024 rotor revolutions to yield the entire periodic-averaged total pressure variation. This averaging ensures that extraneous signals due to turbulent fluctuations and acoustic noise present in the raw signal are averaged out. Figure 20 shows the effect of increasing the number of periods over which a typical signal is averaged. These data indicate that approximately 300 rotor periods are adequate to provide a constant output from the processor.

Table 2

Test Conditions

Test No.	Rotor RPM	Inlet Velocity (ft/sec)	Radial Position (inches)	Axial Position	Inlet Flow	θ_p	θ_c
1	1,600	64.4	7.75	1	Uniform	22°	75°
2	1,601	64.7	7.75	2	Uniform	22°	75°
3	1,601	58.9	7.75	2	Four-Cycle	30°	75°

* refer to Figure 21

** circumferential mean

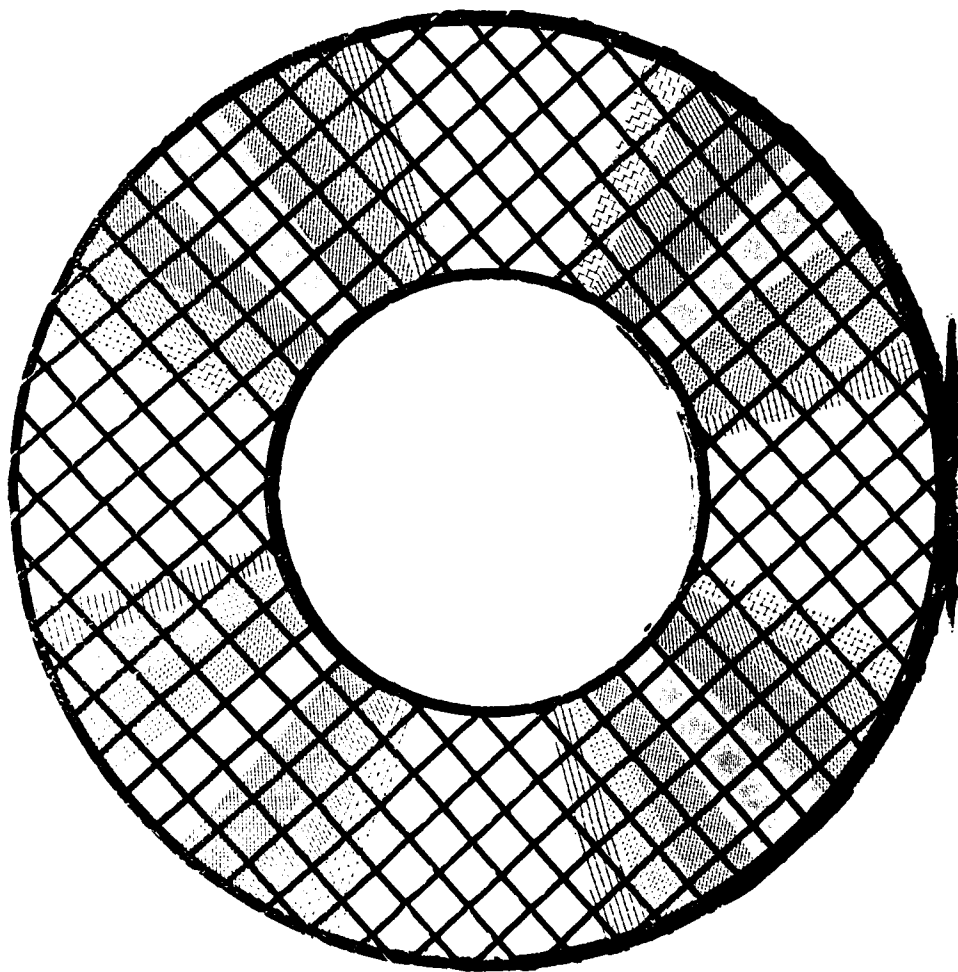


FIGURE 19. FOUR-CYCLE DISTORTION GENERATING SCREEN

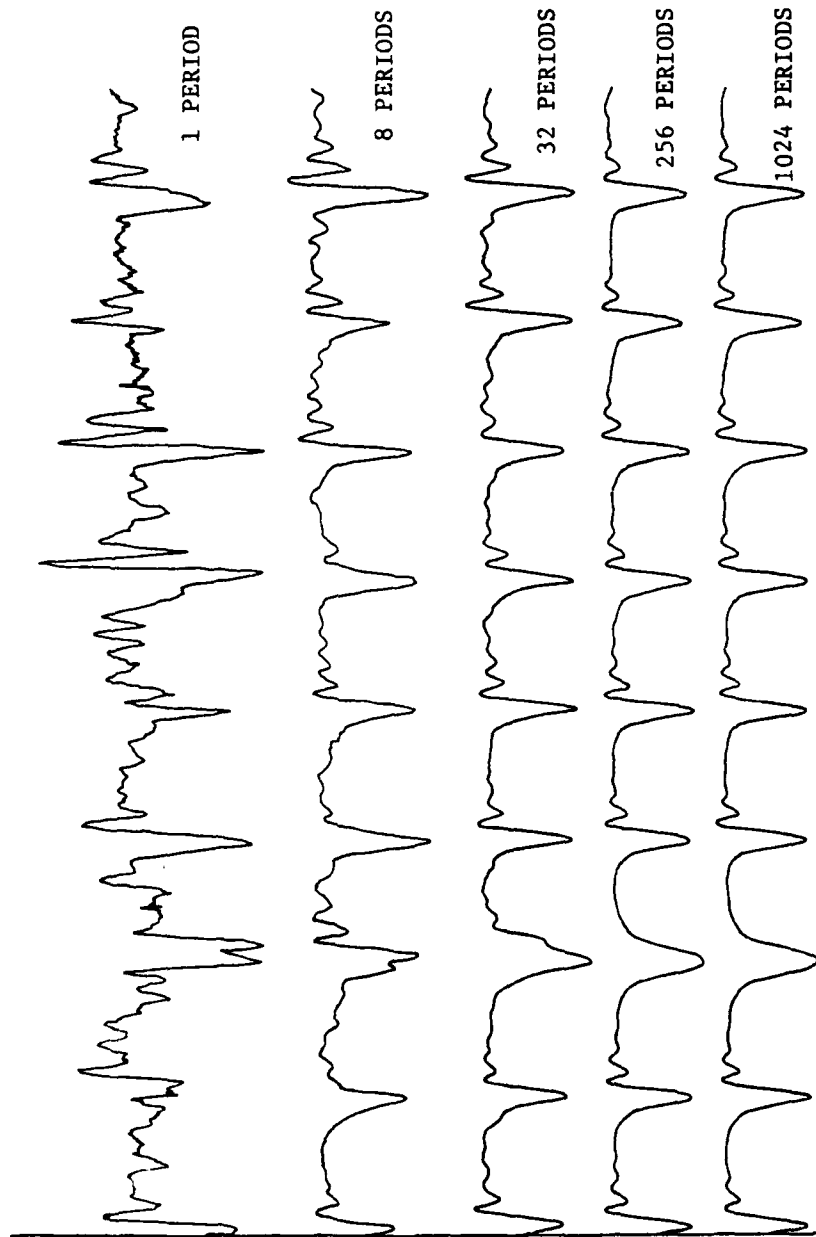


FIGURE 20. THE EFFECT ON A TYPICAL PROBE OUTPUT OF INCREASING THE NUMBER OF ENSEMBLE-AVERAGED PERIODS

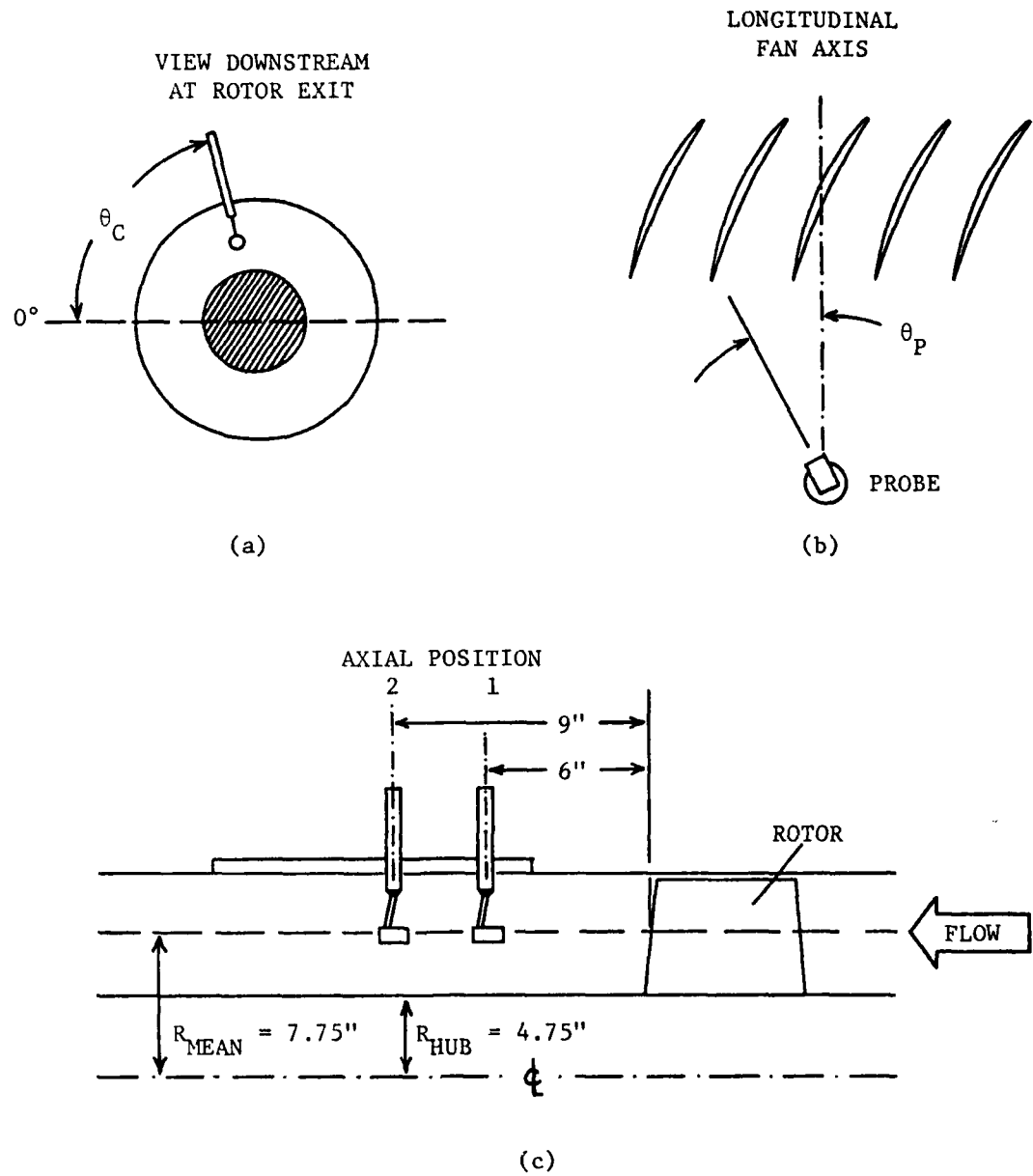


FIGURE 21. PROBE ORIENTATION PARAMETERS: (a) CIRCUMFERENTIAL ANGLE, (b) YAW ANGLE, (c) AXIAL AND RADIAL LOCATIONS

Each ensemble-averaged signal was immediately Fourier analyzed and decomposed into the form

$$X = a_0/2 + \sum_{n=1}^N a_n \cos(2\pi n f_0 t) + b_n \sin(2\pi n f_0 t) \quad , \quad (4)$$

where

X = ensemble-averaged output from signal processor,

$a_0/2$ = time average of signal,

a_n = cosine Fourier coefficient,

b_n = sine Fourier coefficient,

n = harmonic number (1, 2, 3, ... N),

f_0 = fundamental frequency, and

t = time.

The signal was transformed in this manner to allow a correction to be made which accounts for the probe and amplifier response characteristics which modified the ensemble-averaged signal.

Along with fast-response Kiel probe data, total pressure readings were obtained using the standard Kiel probe and a Validyne pressure transducer at the same conditions. (A calibration curve for this transducer (T-2) may be found in the Appendix B.) The value of the total pressure was recorded with the data acquisition system for three consecutive runs, which were used to obtain an averaged value.

Additional data that were recorded for each test consisted of

(1) flow angle indicated by the three-hole wedge probe,

- (2) static pressure in the inlet section,
- (3) rotor rpm (obtained from the data acquisition system),
- (4) rotor rpm (obtained from the tracking ratio tuner),
- (5) fast-response probe zero (before and after each test run),
- (6) fast-response probe excitation voltage,
- (7) ambient temperature, and
- (8) atmospheric pressure.

The earlier problem of DC zero shift of the fast-response Kiel probe was minimized by examination of the shift behavior. At ambient conditions, zero shift was observed to be ± 0.012 mV over a 15-minute period. Immersion of the probe into the AFRF flow field produced a zero shift of the order of one-half millivolt when the probe reached equilibrium. This took approximately one to two minutes. At this point, probe zero did not vary more than the originally observed zero shift. As a result, the following zeroing procedure was adopted. The probe was inserted into the flow and allowed to stabilize for five minutes. It was then removed, zeroed, and immediately returned to the flow. This last step was repeated at half-minute intervals until the difference between two consecutive zero values was less than 0.005 mV. This process usually took less than four repetitions.

DATA REDUCTION

The reduction of the fast-response Kiel probe data involved the modification of the Fourier representation of each signal by the probe's calibration curves and the amplifier's gain and phase shift. This took the form of generating the wave defined as

$$\Delta P = \left(\frac{1}{G} \right) \times (S_1) \times \left[\frac{a_0}{2} + \sum_{n=1}^N \frac{a_n}{c_n} \cos (n\theta + \phi_n) + \frac{b_n}{c_n} \sin (n\theta + \phi_n) \right], \quad (5)$$

with

$$\theta = (2\pi f_o t + \alpha), \quad (6)$$

$$c_n = 10^{(D_n/20)},$$

where

ΔP = total pressure (psig),

G = amplifier gain ($20 \cdot \frac{V}{V}$),

α = amplifier phase lag (π radians),

D_n = measured probe amplitude gain from time-mean (dB),

ϕ_n = measured probe phase lag from time-mean (radians), and

S_1 = probe static sensitivity ($4.01 \times 10^{-3} \frac{\text{psi}}{\text{mV}}$).

The first 60 terms of the Fourier analysis were considered when generating the above wave for each test condition. The values for D_n and ϕ_n were obtained from curve fits of the measured probe response data, Figure 16, and are included in Appendix A.

The standard Kiel probe data were reduced by obtaining the average of three consecutive data readings, multiplying this by the Validyne's sensitivity, and correcting the value for the height difference between probe and transducer:

$$\Delta P = (S_2) \times \left[\frac{1}{3} \sum_{j=1}^3 V_j \right] + \rho g h \quad , \quad (7)$$

where

ΔP = total pressure (psfg),

S_2 = Validyne sensitivity $\left(11.851 \frac{\text{psf}}{\text{V}} \right)$,

V_j = Validyne output voltage (V),

ρ = density of air calculated from the ideal gas equation
(slugs/ft³),

g = acceleration due to gravity (ft/sec²), and

h = height between transducer and probe (4.5 ft).

Finally, all total pressure data were nondimensionalized by forming the following total pressure coefficient:

$$C_{P_t} = \frac{\Delta P}{\frac{1}{2} \rho U^2} \quad , \quad (8)$$

where

ΔP = total pressure (psfg),

ρ = density of air (slugs/ft³), and

U = rotor blade speed at mean radius (fps).

DISCUSSION AND PRESENTATION OF RESULTS

The periodic-averaged total pressure data obtained with the fast-response Kiel probe and the time-averaged total pressure indicated by the standard Kiel probe are presented in this section, along with a plot of the spectral content of a typical fast-response Kiel probe output. The total pressure data are plotted as a nondimensional total pressure coefficient, defined in the previous section.

To give an indication of the raw content of the fast-response probe's output, a plot of the spectral content of a typical output signal for one rotor revolution is given in Figure 22. A large response is seen at the rotor blade passing frequency (BPF) and its multiples. Also quite noticeable is the BPF associated with the auxiliary fan of the AFRF. The auxiliary fan BPF does not appear in the ensemble-averaged data, however, since it is not harmonic with respect to the rotor period.

Figure 23 presents the variation of the ensemble-averaged, but uncorrected for probe dynamic response, pressure coefficient over the time required for one rotor revolution. These data were obtained in a uniform flow and correspond to the first test condition in Table 2. Applying the corrections for the probe's dynamic response, Figure 16, as described by Equation (5), results in the plot of pressure coefficient versus time shown in Figure 24. Also included in Figure 24 are the time-averaged values determined by the standard and fast-response Kiel probes.

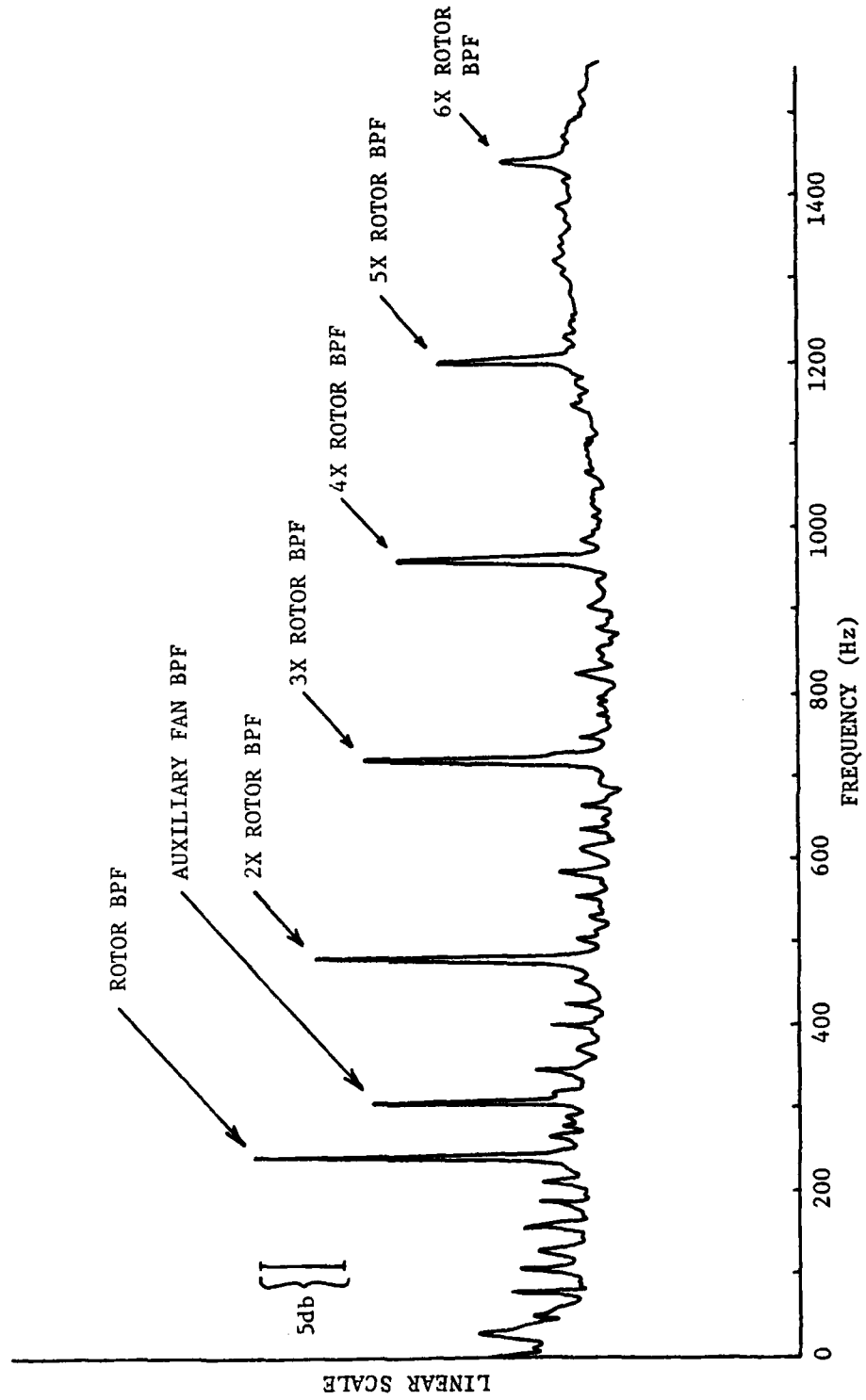


FIGURE 22. SPECTRAL CONTENT OF A TYPICAL FAST-RESPONSE KIEL PROBE OUTPUT FOR ONE ROTOR REVOLUTION

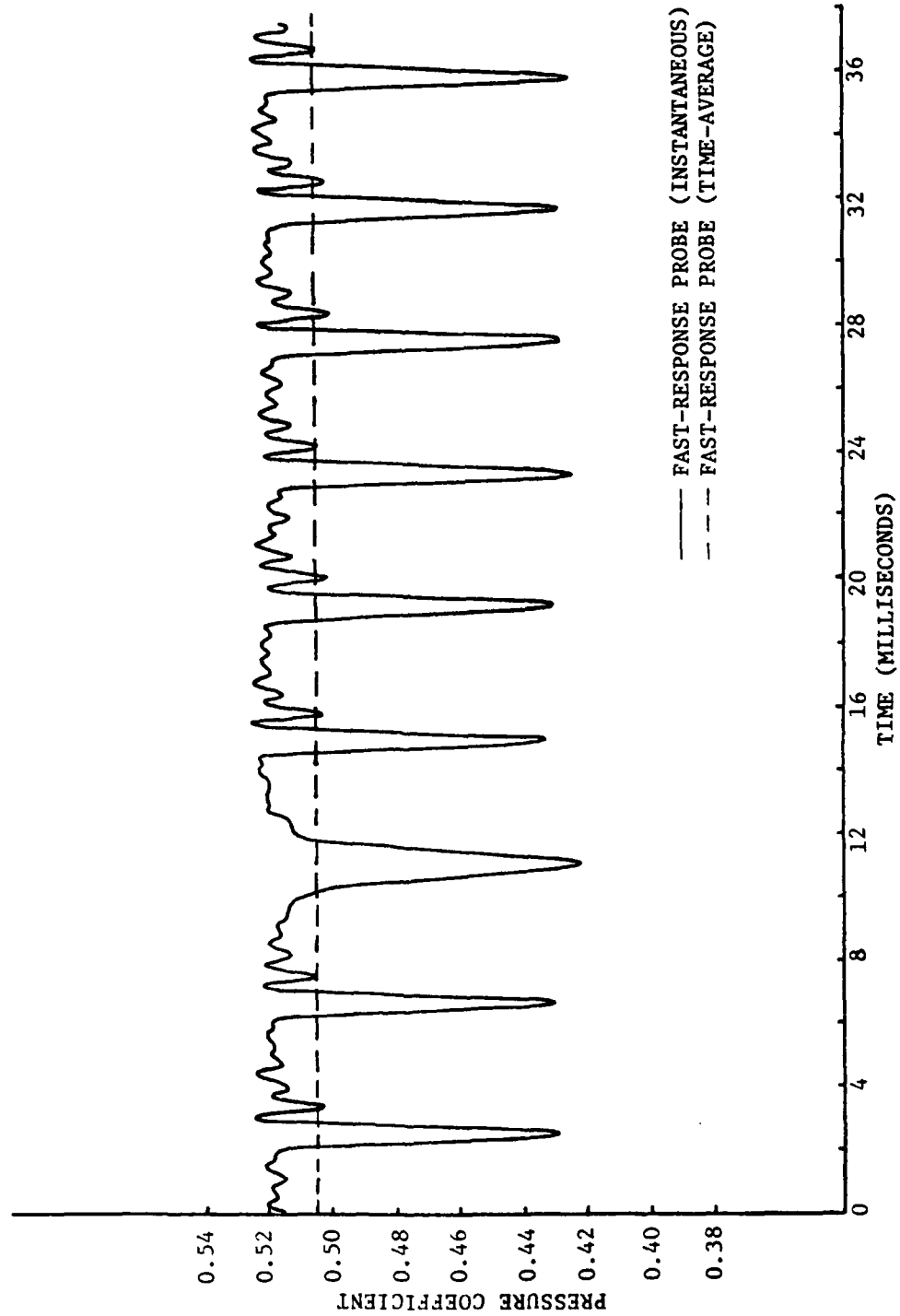


FIGURE 23. PERIODIC VARIATION OF THE ENSEMBLE-AVERAGED TOTAL PRESSURE COEFFICIENT, UNCORRECTED FOR PROBE DYNAMIC RESPONSE, TEST CONDITION NO. 1

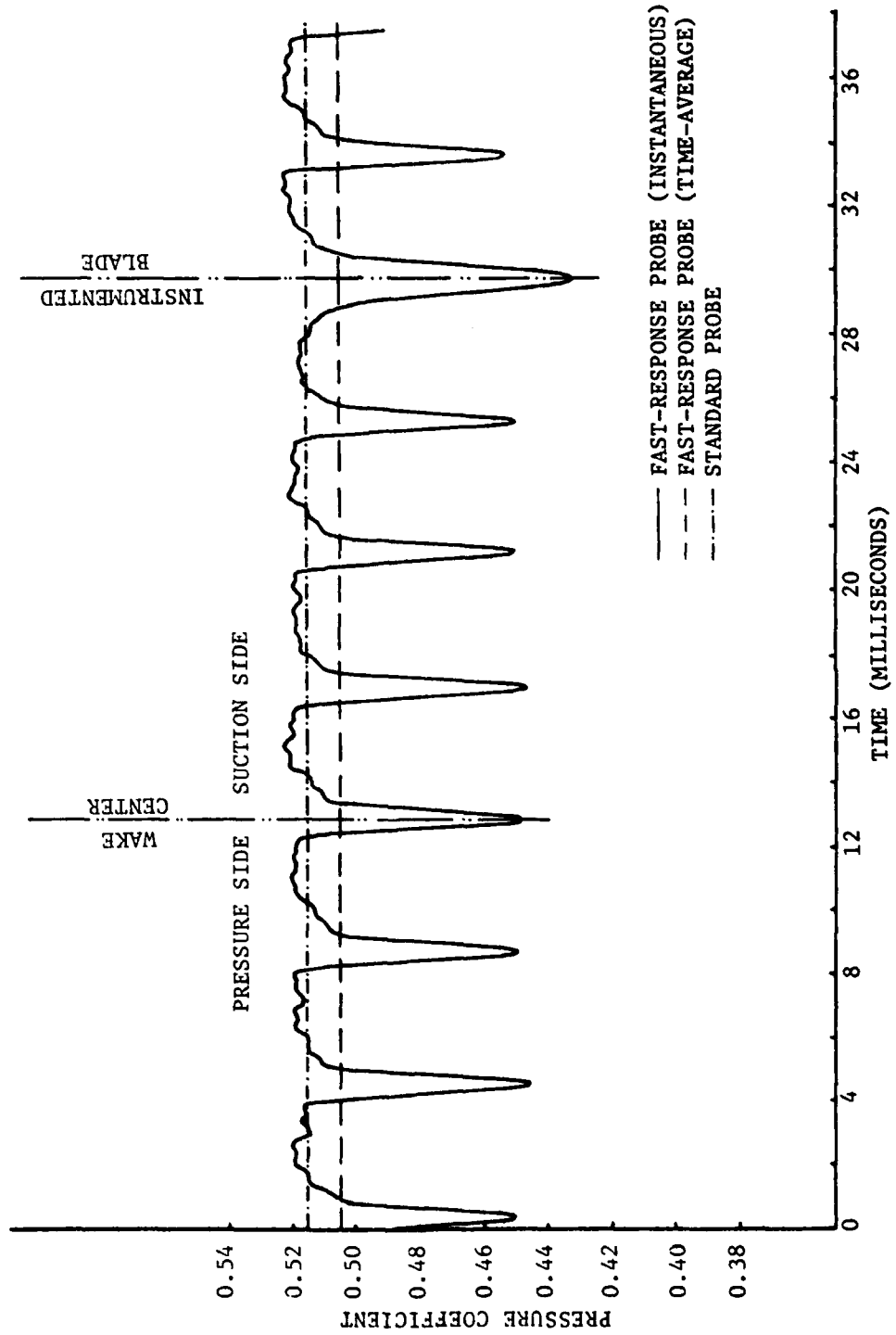


FIGURE 24. PERIODIC VARIATION OF THE ENSEMBLE-AVERAGED TOTAL PRESSURE COEFFICIENT AND THE TIME-AVERAGED VALUE OF THE STANDARD KIEL PROBE, TEST CONDITION NO. 1

A comparison of Figures 23 and 24 clearly shows the dynamic influence of the probe cavity on the actual instantaneous total pressure.

Examination of Figure 24 shows the difference between the total pressure and, hence, the boundary layer development on the suction and pressure sides of the blades. The pressure side of each blade, located to the left of each wake, has a higher total pressure than the suction side of the blade. This indicates a fuller boundary layer at the trailing edge of the pressure side and is consistent with the expected wake shape. The deeper and wider wake observed in Figure 24 (and Figure 23) is due to the rotor blade which is instrumented to measure unsteady rotor lift and moment. The larger total pressure loss associated with this blade is presumably due to the flow leakage around the instrumented segment of this blade.

A comparison of the time-averaged total pressures measured by the fast-response and the standard Kiel probes shows the standard probe to indicate a value 2.1% higher. This difference is due to the inability of the standard Kiel probe to correctly sense the time-averaged value of the fluctuating flow.

The results for the second test, where the probes were placed one-half rotor chord length further downstream (1.5 rotor chord lengths from the rotor trailing edge) at the same flow conditions as the first test, are plotted in Figure 25. These data indicate that the time-mean flow has circumferentially rotated approximately 28° when compared to Figure 24. This is easily seen by the change in position of the wake shed by the instrumented blade. Some of the high frequency fluctuations present in the upstream total pressure trace (Test No. 1) have decreased, and a spatial redistribution of the total pressure has occurred. The latter

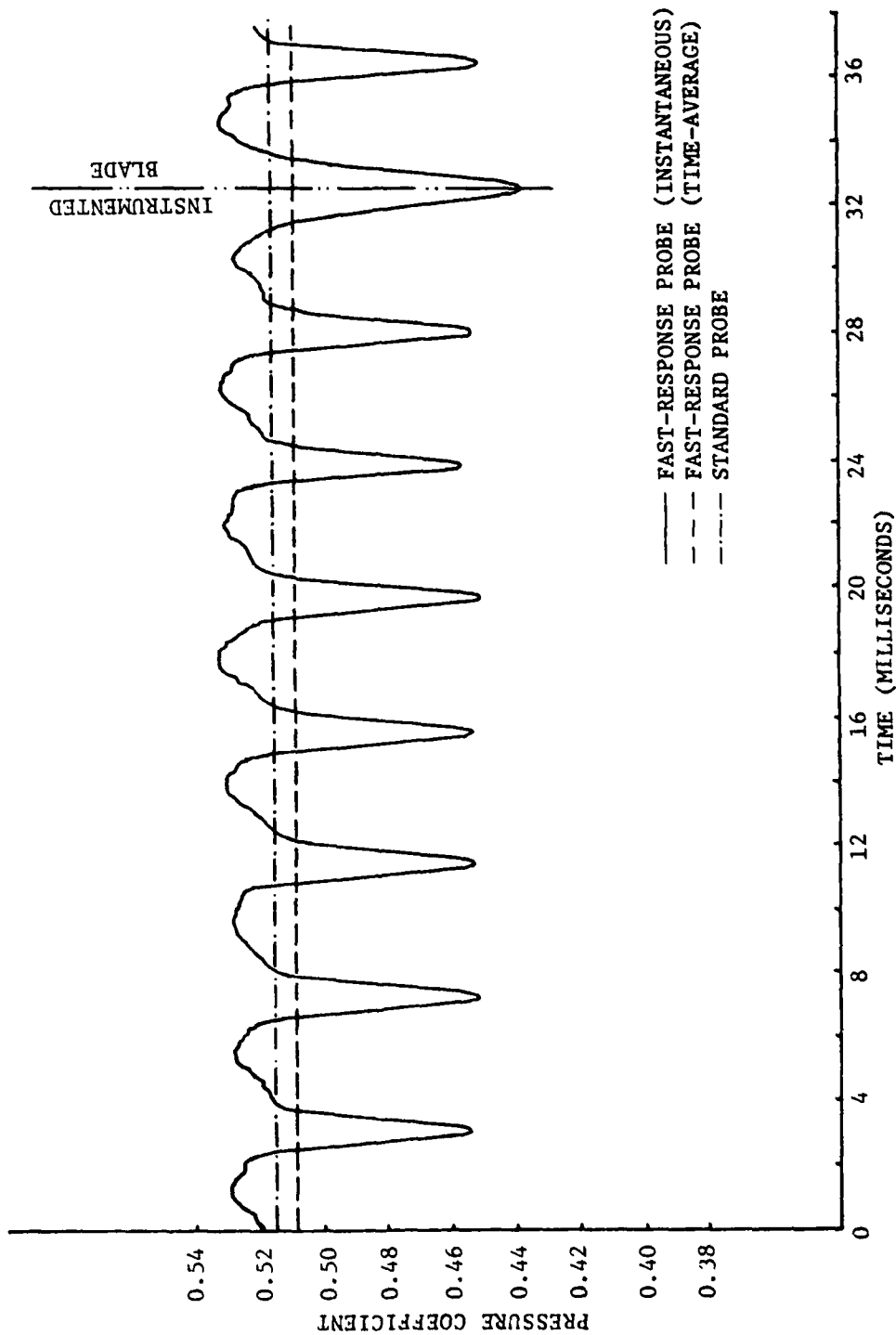


FIGURE 25. PERIODIC VARIATION OF THE ENSEMBLE-AVERAGED TOTAL PRESSURE COEFFICIENT AND THE TIME-AVERAGED VALUE OF THE STANDARD KIEL PROBE, TEST CONDITION NO. 2

characteristic is seen by the widening of the wakes and a slight increase in the magnitude of the total pressure between the wakes, although the pressure and suction sides of the blades are still distinguishable. As shown in Table 3, the time-averaged pressure indicated by the fast-response probe essentially remains constant, while that given by the standard probe shows a slight loss, when compared to their upstream values. In addition, the standard Kiel probe now measures a value for the time-averaged total pressure that is 1.3% higher than the time-averaged value of the fast-response probe. This change in the time-averaged output of the standard probe is the influence of the frequency content of the wakes past the probe. The frequency content has changed due to the spatial redistribution discussed above.

The data obtained during the final test, with the rotor operated in a four-cycle distorted inflow, are shown in Figure 26. The total pressure fluctuations measured downstream of the rotor are the result of the rotor blades passing through this circumferentially varying flow. Figure 27 is a plot of the actual flow field just upstream of the rotor for a mean velocity of 56 ft/sec (27). A schematic of the flow for the given test conditions is shown in Figure 28. As the rotor blades are subjected to varying axial velocities, the flow incidence angle will change. This will cause the rotor blades to experience varying amounts of lift, depending upon the inflow at a particular spatial position. This, in turn, will result in a varying drag and total pressure increase across the rotor. As Figure 26 plainly shows, the existence of unsteady forces on the blades definitely changes the structure of the wakes and, hence, the instantaneous total pressure. The time-averaged total pressure indicated by both probes has decreased, with the standard Kiel probe

Table 3

Comparison of the Time-Averaged Total Pressures
 fo. Test No. 1 and Test No. 2

Test No.	Axial Location	Fast-Response Probe Time-Mean Total Pressure (psfg)	Standard Probe Time-Mean Total Pressure (psfg)	Fast-Response Probe C_{p_t}	Standard Probe C_{p_t}
1	1	6.52	6.65	0.505	0.516
2	2	6.51	6.60	0.509	0.515

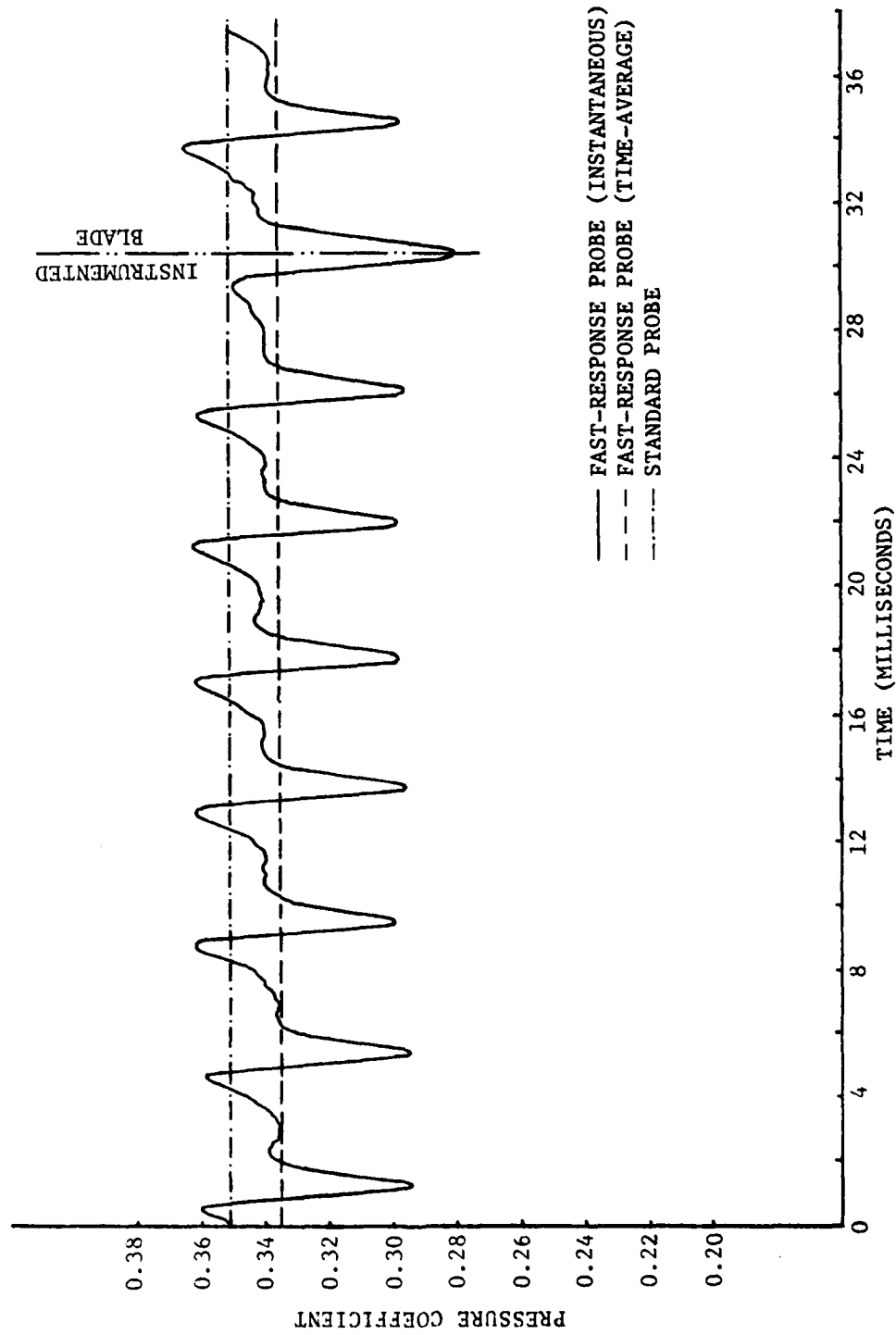


FIGURE 26. PERIODIC VARIATION OF THE ENSEMBLE-AVERAGED TOTAL PRESSURE COEFFICIENT AND THE TIME-AVERAGED VALUE OF THE STANDARD KIEL PROBE, TEST CONDITION NO. 3

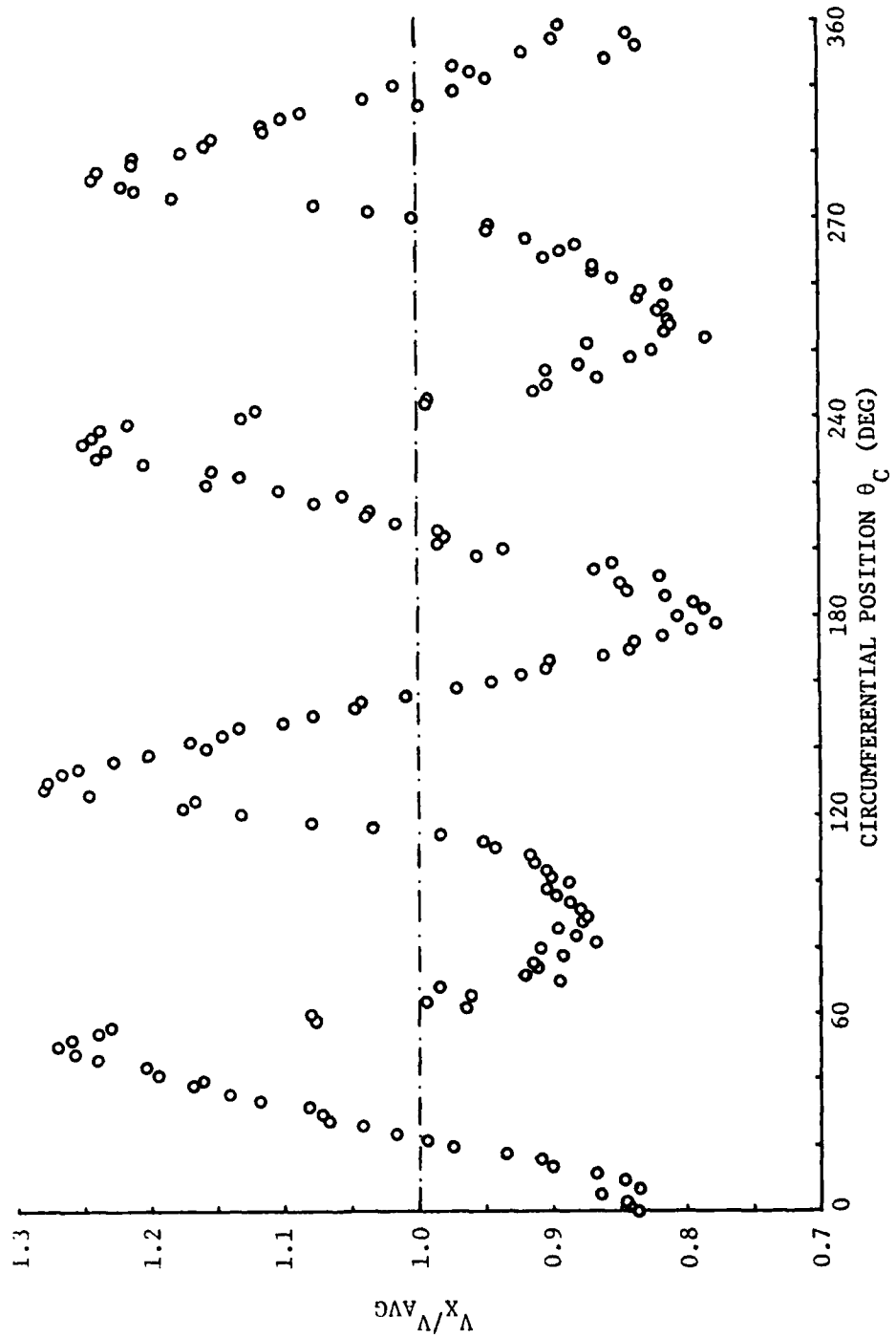


FIGURE 27. AXIAL VELOCITY DISTRIBUTION JUST UPSTREAM OF ROTOR FOR FOUR-CYCLE SCREEN
($V_{AVG} = 56$ FT/SEC)

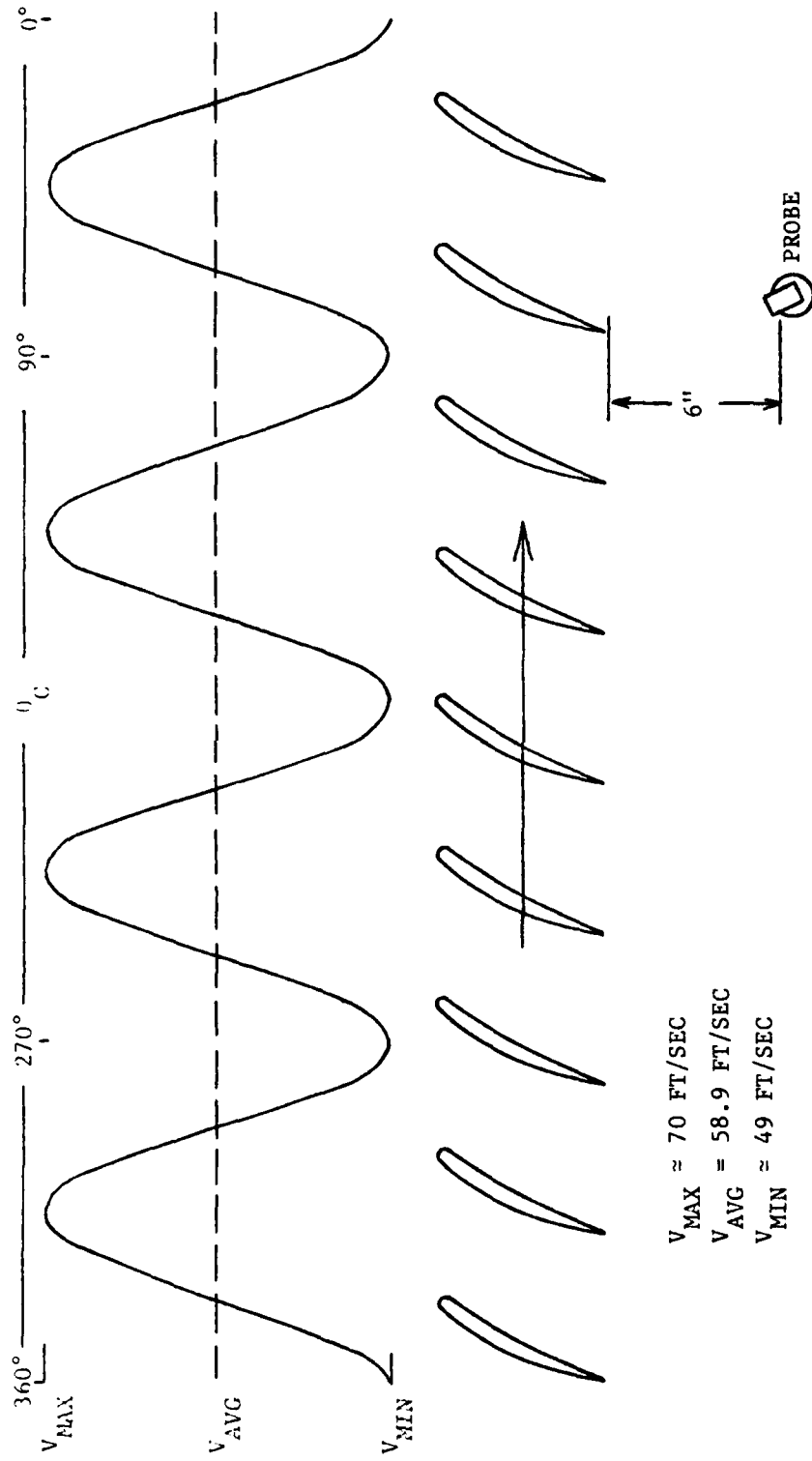


FIGURE 28. SCHEMATIC OF FOUR-CYCLE FLOW DISTORTION SHOWING PROBE POSITION RELATIVE TO FLOW

indicating a time-averaged total pressure 4.7% higher than that given by the fast-response probe.

The relative error associated with the standard and fast-response probe may be estimated from calibration data and/or instrument specifications. The standard Kiel probe measurements have an error of $\pm 0.8\%$, based on calibration data. The time-averaged component of the fast-response Kiel probe has an error of $\pm 1.0\%$, based on calibration data, transducer specifications, and observed zero drift. The instantaneous component of the fast-response Kiel probe has an error of $\pm 5.0\%$, based on probe calibration data.

CHAPTER VI

SUMMARY AND CONCLUSIONS

The purpose of this study was to design, fabricate, and calibrate a fast-response total pressure probe for use in a turbomachine. This was accomplished by using a standard, commercially available, 0.125-inch maximum diameter Kiel probe which was altered to accept a piezo-resistive transducer. The calibration of this arrangement was conducted in a Galton Whistle, which produced a sinusoidal waveform of varying amplitude and frequency. The transducer/cavity/tube arrangement of the probe was simulated for calibration purposes and compared with the response of a known transducer, a 0.25-inch Brüel and Kjaer microphone. The calibrated fast-response Kiel probe was then employed in an axial flow fan and its results compared with a standard 0.125-inch diameter Kiel probe.

As a result of this study, the following conclusions were made:

1. The dynamic response characteristics of a tube/cavity system, such as that employed in the design of a fast-response total pressure probe, can be adequately predicted through the use of the nonlinear analysis of Bergh and Tijdeman (13). The computer program of Bergh and Tijdeman's analysis was obtained from the studies by Nylund, England, and Anderson (14). The predicted and measured resonance frequencies were 1,530 Hz and 1,500 Hz, respectively.

2. The Galton Whistle provides an adequate method for the direct dynamic calibration of the test probe. The large number of sinusoidal waveforms that can be generated without the need of signal conditioning equipment and the simplicity of design make it a satisfactory calibration device.
3. The use of a commercially available Kiel probe in the design of a fast-response total pressure probe greatly reduces construction time and cost, while providing a large insensitivity to flow misalignment. However, the dynamic response of the probe is compromised due to the large connecting volume between the pressure sensing hole and the transducer. This can be compensated for by the direct calibration of the probe.
4. Measurement of both the AC and DC components of the total pressure fluctuation with a single probe is made possible through the use of a temperature compensated piezo-resistive transducer. This temperature compensation minimized thermal sensitivity and DC zero drift. Mechanical contact of the transducer and probe causes a zero shift error, but may be adequately compensated for by a repetitive zeroing procedure.
5. The difference between the time-averaged values for both probes is significant, as high as 4.7%, due to frequency dependent effects. The inability of a standard Kiel probe to accurately measure the time-averaged value of a total pressure fluctuation makes

a fast-response probe very valuable. The error associated with the fast-response probe measurements was determined to be $\pm 1.0\%$ for the DC component and $\pm 5.0\%$ for the AC component.

6. The employment of the fast-response total pressure Kiel probe at the exit of an axial flow rotor clearly shows that minute details, such as the differences in the boundary layer on the pressure and suction surfaces, can be observed. Furthermore, the operation of the rotor in a spatially varying inflow results in a significantly different wake than observed in a uniform inflow.

CHAPTER VII

RECOMMENDATIONS FOR FURTHER RESEARCH

The present effort has resulted in the successful design, construction, and calibration of an instantaneous total pressure probe. Future efforts should seek further refinements in the probe design, such as providing a high resonant frequency, and make application of this probe to the study of rotor wake flows for the rotor in both a uniform and spatially varying inflow. Specific recommendations include:

1. The elimination of probe/transducer contact to remove any zero shifting effects caused by it. This may be accomplished by removal of the lip that the base of the transducer rests upon and securing the transducer in place with sealant.
2. A redesigning of the probe head to improve response characteristics. This may be achieved by the design and construction of a probe head that has a shorter tubing length in its tube/cavity configuration, as well as a larger tube radius.
3. Circumferential surveys of the flow before and after the rotor should be attempted with different rotor inflow distortions. Such experiments would serve to demonstrate the effects of unsteady rotor forces on the wake characteristics.

REFERENCES

1. Yocum, A. M., and R. E. Henderson, "The Effects of Some Design Parameters of an Isolated Rotor on Inlet Flow Distortions," ASME Paper No. 79-JT-93, March 1979.
2. Franke, G. F., "Investigation of the Unsteady Pressure Distribution on the Blades of an Axial Flow Fan," Master of Science Thesis, Department of Mechanical Engineering, The Pennsylvania State University, May 1979.
3. Bruce, E. P., and R. E. Henderson, "Axial Flow Rotor Unsteady Response to Circumferential Inflow Distortions," Project SQUID Technical Report PSU-13-P, 1975.
4. Taback, I., "The Response of Pressure Measuring Systems to Oscillating Pressures," NACA TN 1819, 1949.
5. Rayleigh, (Lord), The Theory of Sound, Second Edition, London, Macmillan, 1896.
6. Holman, J. P., Experimental Methods for Engineers, New York, McGraw-Hill, 1966.
7. Doebelin, E. O., Measurement Systems Application and Design, New York, McGraw-Hill, 1966.
8. Delio, G. J., et al., "Transient Behavior of Lumped-Constant Systems for Sensing Gas Pressures," NACA TN 1988, 1949.
9. Alster, M., "Improved Calculation of Resonant Frequencies of Helmholtz Resonators," Journal of Sound and Vibration, 24, 63-85, 1972.
10. Atkins, G. B., "Development and Calibration of a Probe/Sensor System to Measure Instantaneous Total Pressures," Thesis in Aerospace Engineering for the Degree of Bachelor of Science, The Pennsylvania State University, University Park, PA, 1974.
11. Atkins, G. B., "On the Development and Calibration of a Fast-Response Probe/Sensor System to Measure Instantaneous Total Pressures," Applied Research Laboratory Technical Memorandum No. 74-75, April 1974.
12. Iberall, A. S., "Attenuation of Oscillatory Pressure in Instrument Lines," National Bureau of Standards Journal of Research, 45, No. 1, 85-108, 1950.

13. Bergh, H., and H. Tijdeman, "Theoretical and Experimental Results for the Dynamic Response of Pressure Measuring Systems," Report NLR-TR-F28, National Aeronautical and Astronautical Research Institute, Amsterdam, 1965.
14. Nyland, T. W., D. R. Englund, and R. C. Anderson, "On the Dynamics of Short Pressure Probes: Some Design Factors Affecting Frequency Response," NASA TND-6151, 1971.
15. Samoilovich, G. S., and L. D. Yablokov, "Measurement of Periodically Fluctuating Flows in Turbomachines by Ordinary Pitot Tubes," Thermal Engineering, 17, No. 9, 105-110, 1971.
16. Kronauer, R. E., and H. P. Grant, "Pressure Probe Response in Fluctuating Flow," Proceedings 2nd U. S. Congress of Applied Mechanics, 763-770, 1954.
17. Krause, L. N., J. J. Dudzinski, and R. C. Johnson, "Total-Pressure Averaging in Pulsating Flows," NASA TMX-68128, 1972.
18. Davis, E. L., "The Measurement of Unsteady Pressures in Wind Tunnels," AGARD Report, No. 169, 1958.
19. Strasberg, M., "Measurement of Fluctuating Static and Total-Head Pressure in a Turbulent Wake," AGARD Report, No. 464, 1963.
20. Siddon, T. E., "On the Response of Pressure Measuring Instrumentation in Unsteady Flow," University of Toronto Institute of Aerospace Sciences Report No. 136, 1969.
21. Armentrout, E. C., "Development of a High Frequency Response Pressure Sensing Rake for Turbofan Engine Tests," NASA TMX-1959, 1970.
22. Senoo, Y., Y. Kita, and K. Ookuma, "Measurement of Two-Dimensional Periodic Flow with a Cobra Probe," ASME Journal of Fluids Engineering, June 1973.
23. Alarcon, G. A., T. H. Okiishi, and G. H. Junkhan, "Design and Application of a Fast-Response Total Pressure Probe for Turbo-Machinery Flow Measurement," ISU-ERI-AMES-78205, TCRL-9, Project 1204, 1977.
24. Gettelman, C. C., and L. N. Krause, "Considerations Entering into the Selection of Probes for Pressure Measurement in Jet Engines," ISA Proceedings, 7, 135-137, 1952.
25. Nyland, T. W., D. R. Englund, and V. D. Gebben, "System for Testing Pressure Probes Using a Simple Sinusoidal Pressure Generator," NASA TMX-1981, 1970.

26. Bruce, E. P., "The ARL Axial Flow Research Fan - A New Facility for Investigation of Time-Dependent Turbomachinery Flows," ASME Paper No. 74-FE-27, 1974.
27. Consultations with E. P. Bruce at the Applied Research Laboratory, The Pennsylvania State University, May 1978.

APPENDIX A
THEORETICAL AND EXPERIMENTAL EVALUATION OF
TUBE/CAVITY SYSTEM RESPONSE

This section contains the theoretically and experimentally obtained frequency response characteristics of the fast-response total pressure Kiel probe. The theoretical formulation of Bergh and Tijdeman (13), which was employed to predict the probe's frequency response, is presented first. Next, the predictive response data generated by Nyland, Englund, and Anderson's (14) computer program of Bergh and Tijdeman's formulation (restricted to a single tube/cavity system) is given. Finally, the actual response data for the fast-response Kiel probe simulator, as well as their curve fitting equations, are listed.

BERGH AND TIJDEMAN'S MODEL OF TUBE/CAVITY SYSTEM RESPONSE

$$\frac{P_1}{P_0} = \left[\cosh(\phi L) + \frac{V_v}{V_t} \left(\sigma + \frac{1}{K} \right) n \phi L \sinh(\phi L) \right]^{-1},$$

$$\phi = \frac{v}{a_0} \sqrt{\frac{J_0(\alpha)}{J_2(\alpha)}} \sqrt{\frac{\gamma}{n}},$$

$$\alpha = i \sqrt{i} R \sqrt{\frac{\rho_s v}{\mu}},$$

and

$$n = \left[1 + \frac{\gamma-1}{\gamma} \frac{J_2(\alpha \sqrt{P_r})}{J_0(\alpha \sqrt{P_r})} \right]^{-1},$$

where

$\frac{P_1}{P_0}$ = complex pressure ratio,

a_0 = mean velocity of sound,

γ = specific heat ratio (C_p/C_v),

R = tube radius,

L = tube length,

V_v = cavity volume,

V_t = tube volume,

σ = dimensionless increase in transducer volume due to diaphragm deflection,

v = frequency,

K = polytropic constant,

μ = absolute fluid viscosity,

ρ_s = mean density,

J_n = Bessel function of the first kind of order n , and

P_r = Prandtl number.

FAST-RESPONSE KIEL PROBE PREDICTIVE FREQUENCY RESPONSE DATA

Cavity Radius = 0.12700 (CM)	Pressure = 1008703.0 (DYNE/CM**2)
Cavity Length = 0.19830 (CM)	Density = 0.0011790 (GM/CM**3)
Tube Radius = 0.02540 (CM)	Viscosity = 0.0001780 (GM/CM*SEC)
Tube Length = 1.90500 (CM)	Prandtl No. = 0.700
Sigma = 0.00	Gamma = 1.40
Volume Ratio (VC/VT) = 2.602	K = 1.40

	<u>Frequency (CPS)</u>	<u>Amplitude Ratio</u>	<u>Phase Angle (DEG)</u>
	0.00	0.99	0.00
	100.00	1.00	-0.68
	200.00	1.02	-1.41
	300.00	1.04	-2.23
	400.00	1.08	-3.18
	500.00	1.13	-4.31
	600.00	1.20	-5.66
	700.00	1.29	-7.33
	800.00	1.41	-9.42
	900.00	1.57	-12.12
	1000.00	1.78	-15.71
	1100.00	2.07	-20.73
	1200.00	2.49	-28.11
	1300.00	3.07	-39.63
	1350.00	3.42	-47.79
	1400.00	3.76	-58.02
	1450.00	4.01	-70.32
RESONANCE →	1500.00	4.08	-84.03 ←
	1550.00	3.92	-97.74
	1600.00	3.59	-110.08
	1650.00	3.19	-120.34
	1750.00	2.46	-135.00
	1850.00	1.92	-144.21
	1950.00	1.55	-150.29
	2050.00	1.28	-154.55
	2150.00	1.09	-157.69
	2250.00	0.94	-160.11
	2350.00	0.82	-162.04
	2450.00	0.73	-163.63
	2550.00	0.66	-164.96
	2650.00	0.59	-166.10
	2750.00	0.54	-167.10

CALIBRATION DATA FOR FAST-RESPONSE PROBE

RUN NO. 1

<u>Frequency (Hz)</u>	<u>Phase Lag (DEG)</u>	<u>Amplitude Gain (dB)</u>
0	0.0	0.0
314	6.82	0.684
504	8.67	1.074
652	8.94	2.150
806	11.56	3.306
950	17.51	4.795
1044	23.27	5.957
1162	34.16	7.438
1312	54.13	9.302
1452	81.53	9.794
1569	106.11	9.115

RUN NO. 2

<u>Frequency (Hz)</u>	<u>Phase Lag (DEG)</u>	<u>Amplitude Gain (dB)</u>
0	0.0	0.0
313	6.62	0.698
504	8.77	1.104
652	8.84	2.197
805	11.36	3.178
949	17.31	4.872
1046	23.25	5.984
1161	33.86	7.353
1312	53.83	9.214
1451	81.23	9.729
1569	106.10	9.115

CURVE FIT EQUATIONS OF RUN NO. 1 DATA

Amplitude Response

For 0 - 1200 Hz:

$$D_n = 2.940 \times 10^{-2} + 4.1883 \times 10^{-4} f + 3.145 \times 10^{-6} f^2 \\ + 1.7444 \times 10^{-8} f^3 .$$

For 1200 - 1600 Hz:

$$D_n = 2.9388 \times 10^1 + 3.1051 \times 10^{-2} f + 1.3958 \times 10^{-5} f^2 \\ - 1.1542 \times 10^{-8} f^3 ,$$

where

$$D_n = \text{Amplitude Gain (dB)} = 20 \log c_n \text{ and}$$

f = Frequency (Hz).

Phase Lag

For 0 - 1200 Hz:

$$\phi_n = \arctan \left(\frac{(1.672 \times 10^{-4}) / (1 - f^2 / 1.9321 \times 10^6)}{+ 2.7433 \times 10^{-2}} \right) .$$

For 1200 - 1600 Hz:

$$\phi_n = 9.4608 \times 10^1 - 2.2296 \times 10^{-1} f + 1.4691 \times 10^{-4} f^2 ,$$

where

ϕ_n = Phase Lag (DEG) and

f = Frequency (Hz).

APPENDIX B
MISCELLANEOUS CALIBRATION DATA

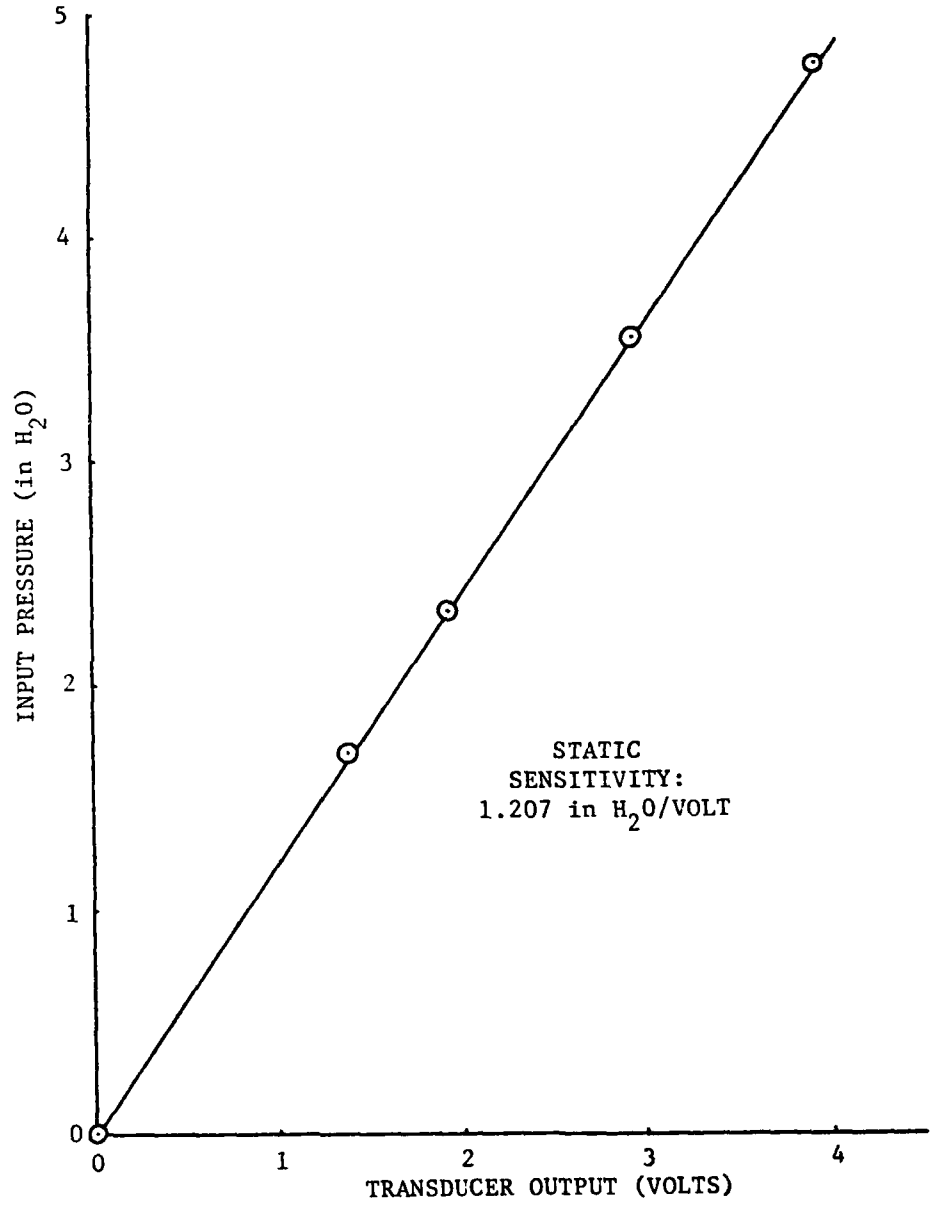


FIGURE B-1. STATIC CALIBRATION OF TRANSDUCER T-1

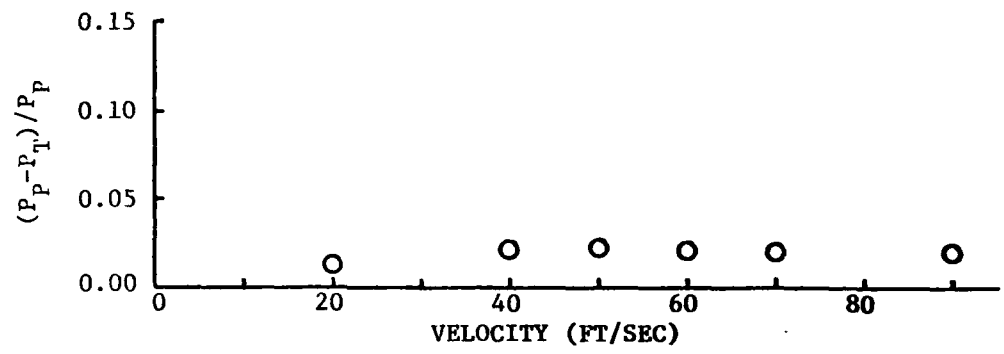


FIGURE B-2. RERUN OF REYNOLDS NUMBER CALIBRATION FOR THE STANDARD KIEL PROBE

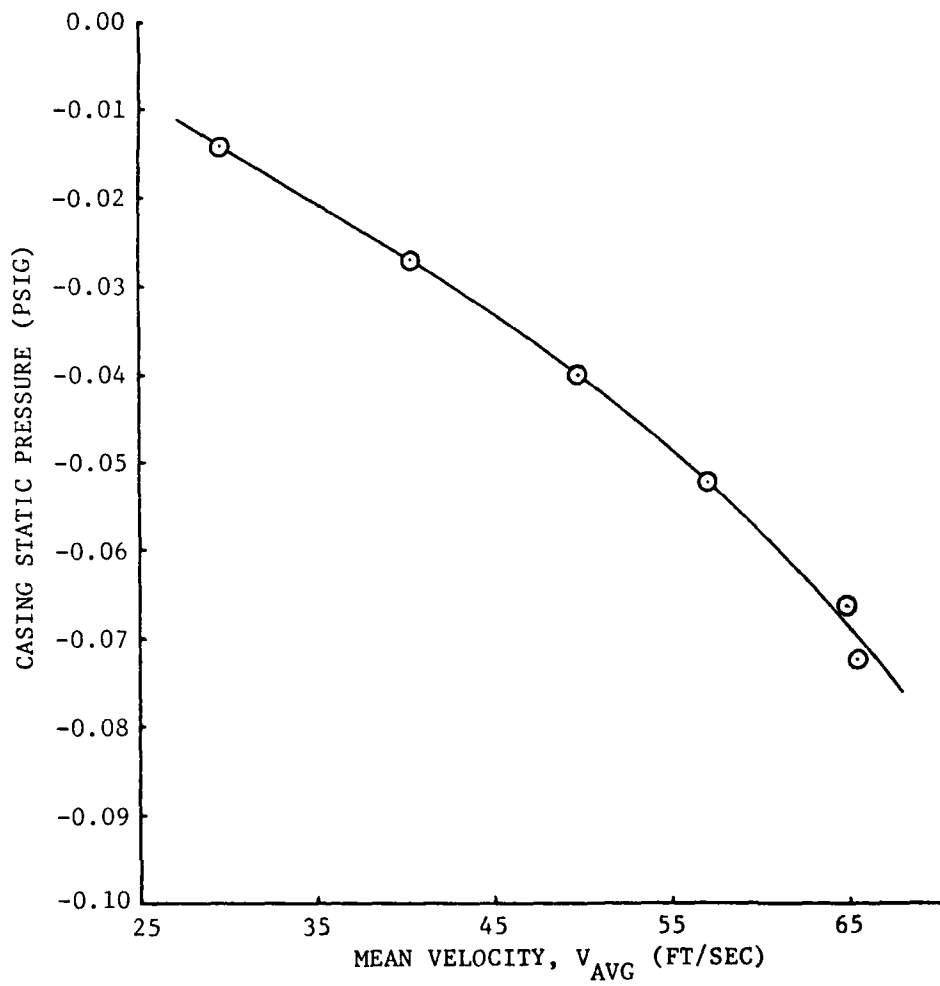


FIGURE B-3. CALIBRATION DATA RELATING V_{AVG} AND CASING STATIC PRESSURE FOR A FOUR-CYCLE DISTORTED INFLOW AT R_{MEAN}

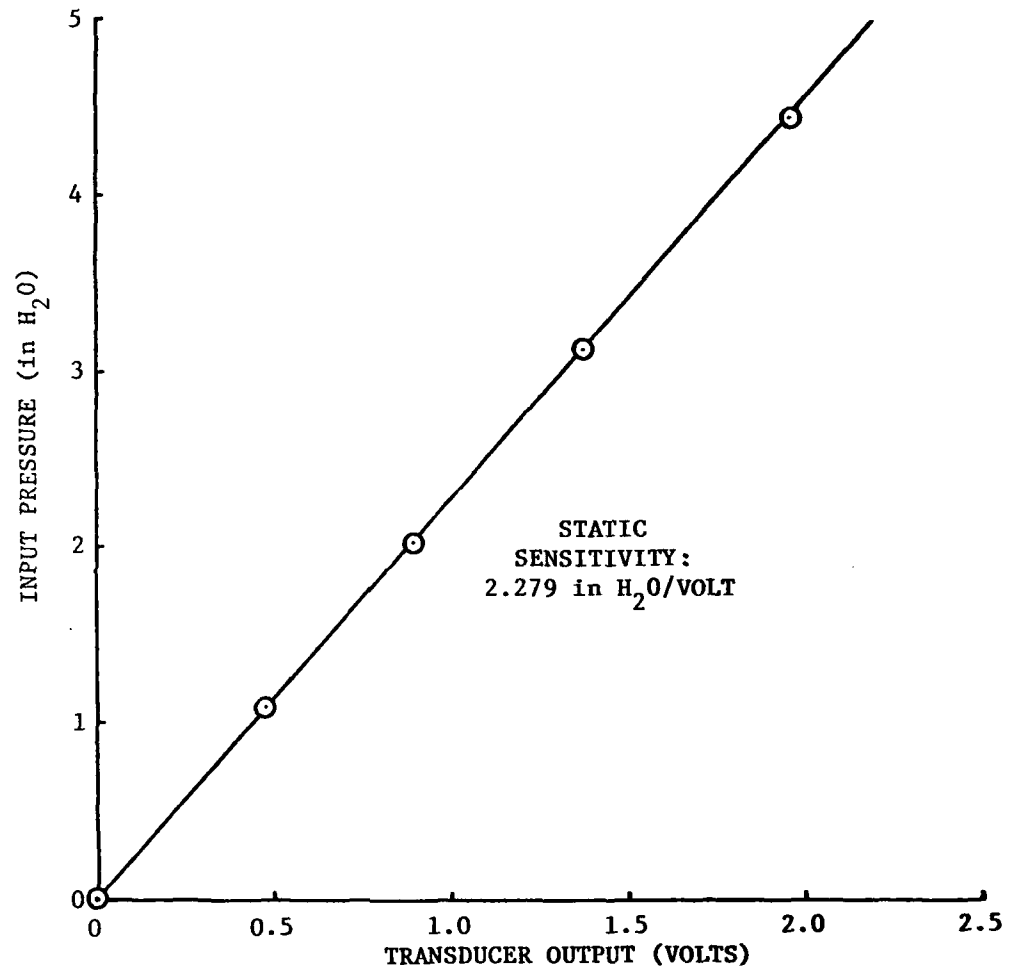


FIGURE B-4. STATIC CALIBRATION OF TRANSDUCER T-2

DISTRIBUTION LIST FOR ARL UNCLASSIFIED TM 79-182 by J. A. Spivak dated
22 October 1979.

Commander
Naval Sea Systems Command
Department of the Navy
Washington, DC 20362
Attn: Library
Code NSEA 09G32
(Copy Nos. 1 and 2)

Naval Sea Systems Command
Attn: Code NSEA 0342
(Copy Nos. 3 and 4)

Naval Sea Systems Command
Attn: T. E. Peirce
Code NSEA 63R3
(Copy No. 5)

Naval Sea Systems Command
Attn: A. R. Paladino
Code NSEA 05H1
(Copy No. 6)

Naval Sea Systems Command
Attn: F. Peterson
Code NSEA 52P
(Copy No. 7)

Defense Technical Information Center
5010 Duke Street
Cameron Station
Alexandria, VA 22314
(Copy Nos. 8 through 19)

Commanding Officer
Naval Underwater Systems Center
Newport, RI 02840
Attn: Library
Code 54
(Copy No. 20)

Commanding Officer
Naval Ocean Systems Center
San Diego, CA 92152
Attn: M. Reischman
Code 2542
(Copy No. 21)

Commanding Officer & Director
David W. Taylor Naval Ship R&D Center
Department of the Navy
Bethesda, MD 20084
Attn: W. B. Morgan
Code 15
(Copy No. 22)

David W. Taylor Naval Ship R&D Center
Attn: R. Cumming
Code 1544
(Copy No. 23)

David W. Taylor Naval Ship R&D Center
Attn: J. H. McCarthy
Code 154
(Copy No. 24)

David W. Taylor Naval Ship R&D Center
Attn: M. Sevik
Code 19
(Copy No. 25)

David W. Taylor Naval Ship R&D Center
Attn: W. K. Blake
Code 1942
(Copy No. 26)

Commanding Officer & Director
David W. Taylor Naval Ship R&D Center
Department of the Navy
Annapolis Laboratory
Annapolis, MD 20084
Attn: J. G. Stricker
Code 2721
(Copy No. 27)

David W. Taylor Naval Ship R&D Center
Attn: Y-F Wang
Code 2740
(Copy No. 28)

Air Force Office of Scientific Research
Bolling Air Force Base, Building 410
Washington, DC 20332
Attn: Dr. Joseph F. Masi
(Copy No. 29)

Office of Naval Research Branch Office
1030 East Green Street
Pasadena, CA 91106
Attn: Dr. Rudolph J. Marcus
(Copy No. 30)

Office of Naval Research Branch Office
536 South Clark Street
Chicago, IL 60605
Attn: Commander
(Copy No. 31)

DISTRIBUTION LIST FOR ARL UNCLASSIFIED TM 79-182 by J. A. Spivak dated
22 October 1979.

Office of Naval Research Branch Office
495 Summer Street
Boston, MA 02210
Attn: Commander
(Copy No. 32)

Office of Naval Research
Power Branch
Department of the Navy
Arlington, VA 22217
Attn: Mr. J. R. Patton
(Copy No. 33)

Office of Naval Research
Fluid Dynamics Branch, Code 438
Department of the Navy
Washington, DC 22217
Attn: Mr. R. D. Cooper
(Copy No. 34)

General Electric Company
AEG Technical Information Center
Mail Drop N-32, Building 700
Cincinnati, OH 45215
Attn: J. J. Brady
(Copy No. 35)

General Motors Corporation
Detroit Diesel Allison Division
P.O. Box 894
Indianapolis, IN 46206
Attn: Mr. P. C. Tram
(Copy No. 36)

Pratt and Whitney Aircraft
Project Engineer, Advanced
Military System
Engineering Department - 2B
East Hartford, CT 06108
Attn: Mr. Donald S. Rudolph
(Copy No. 37)

Pratt and Whitney Aircraft
Florida Research and Development Company
P.O. Box 2691
West Palm Beach, FL 33402
Attn: Mr. William R. Alley
Chief of Applied Research
(Copy No. 38)

United Technologies Research Center
400 Main Street
East Hartford, CT 06108
Attn: Mr. Franklin O. Carta
(Copy No. 39)

Massachusetts Institute of Technology
77 Massachusetts Avenue
Cambridge, MA 02139
Attn: Dr. E. M. Greitzer
(Copy No. 40)

Stevens Institute of Technology
Department of Mechanical Engineering
Castle Point Station
Hoboken, NJ 07030
Attn: Professor F. Sisto
(Copy No. 41)

ONERA
Energie and Propulsion
29 Avenue de la Division Leclure
92 Chatillon sous Bagneux, FRANCE
Attn: Mr. J. Fabri
(Copy No. 42)

Virginia Polytechnic Institute and State
University
Mechanical Engineering Department
Blacksburg, VA 24601
Attn: Dr. Walter F. O'Brien, Jr.
(Copy No. 43)

Purdue University
School of Aeronautics and Astronautics
Grissom Hall
West Lafayette, IN 47907
Attn: Library
(Copy No. 44)

Purdue University
Chaffee Hall
Attn: Dr. S. N. B. Murthy
(Copy No. 45)

Purdue University
Attn: Dr. S. Fleeter
(Copy No. 46)

University of Salford
Salford, M5 4WT
ENGLAND
Attn: Dr. John H. Horlock
Vice Chancellor
(Copy No. 47)

Netherlands Ship Model Basin
P.O. Box 28
6700 AA Wageningen
THE NETHERLANDS
Attn: Dr. P. van Oossanen
(Copy No. 48)

DISTRIBUTION LIST FOR ARL UNCLASSIFIED TM 79-182 by J. A. Spivak dated
22 October 1979.

Mut-Munchen GmbH
8 Munchen 50
Postfach 50 06 40
GERMANY

Attn: Dr. Hans Mokolke
(Copy No. 49)

Forschungsbeauftragter für Hydroakustik
8012 Ottobrunn B. Munchen
Waldparkstr. 41
Munich
GERMANY

Attn: Dr. rer. nat. Horst Merbt
(Copy No. 50)

Admiralty Marine Technology Establishment
Teddington, Middlesex
ENGLAND

Attn: Dr. Allen Moore
(Copy No. 51)

Whittle Turbomachine Laboratory
Madingley Road
Cambridge
ENGLAND

Attn: Dr. D. S. Whitehead
(Copy No. 52)

Whittle Turbomachine Laboratory
Attn: Library
(Copy No. 53)

Von-Karman Institute for Fluid Dynamics
Turbomachinery Laboratory
Rhode-Saint-Genese
BELGIUM

Attn: Library
(Copy No. 54)

Turbine Research Department
Rolls Royce Ltd.
P. O. Box 31
Derby
ENGLAND

Attn: Dr. D. S. Thompson
(Copy No. 55)

NASA Lewis Research Center
21000 Brookpark Road
Cleveland, OH 44135
Attn: J. Adamczyk
MS 5-9
(Copy No. 56)

NASA Lewis Research Center
Attn: W. M. McNally
MS 5-9
(Copy No. 57)

Cranfield Institute of Technology
School of Mechanical Engineering
Cranfield, Bedford MK430AL
ENGLAND

Attn: Professor R. E. Peacock
(Copy No. 58)

Iowa State University
Mechanical Engineering Department
Ames, IA 50010

Attn: Dr. T. H. Okiishi
(Copy No. 59)

NASA Ames Research Center
Moffett Field, CA 94085
Attn: Dr. S. Bodapati
MA 227-9
(Copy No. 60)

Allis-Chalmers Corporation
Hydro-Turbine Division
Box 712
York, PA 17405
Attn: R. K. Fisher
(Copy No. 61)

NSW Institute of Technology
School of Mechanical Engineering
Broadway
Sidney
AUSTRALIA
Attn: Professor J. P. Gostelow
(Copy No. 62)

U.S. Naval Air Propulsion Center
1440 Parkway Avenue
Trenton, NJ 08628
Attn: Donald Brunda
(Copy No. 63)

Naval Post Graduate School
Department of Aeronautics
Monterey, CA 93940
Attn: Dr. M. F. Platzler
(Copy No. 64)

AD-A091 157

PENNSYLVANIA STATE UNIV UNIVERSITY PARK APPLIED RESE--ETC F/6 14/2
DEVELOPMENT OF A FAST-RESPONSE TOTAL PRESSURE PROBE FOR USE IN --ETC(U)
OCT 79 J A SPIVAK N00014-75-C-1143
ARL/PSU-TM-79-182 NL

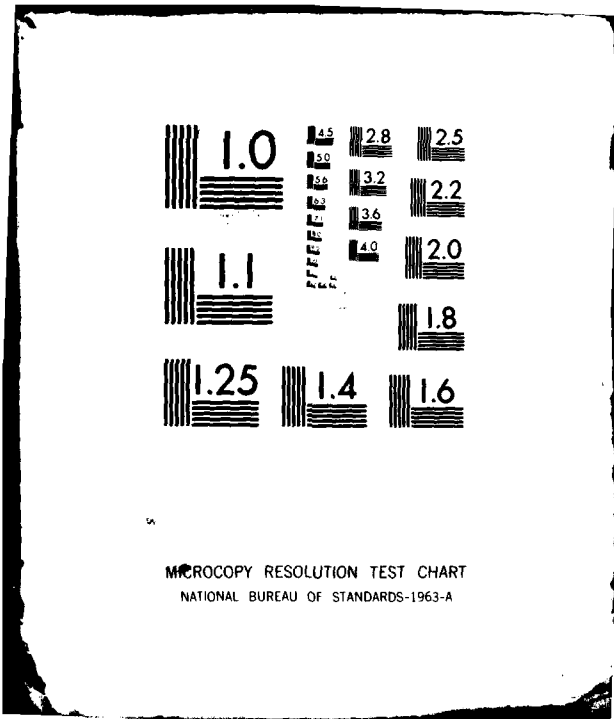
UNCLASSIFIED

2 of 2

AD-A091 157



END
DATE
FILMED
12 80
DTIC



MICROCOPY RESOLUTION TEST CHART
NATIONAL BUREAU OF STANDARDS-1963-A

DISTRIBUTION LIST FOR ARL UNCLASSIFIED TM 79-182 by J. A. Spivak dated
22 October 1979.

Institute for Turbomachines
Technical University
Templergraben 55
D-5100 Aachen
Federal Republic of Germany
Attn: Dr. H. Gallus
(Copy No. 65)

HSVA Gmbh
Bramfelder Strasse 164
200 Hamburg 60
Postfach 600 929
Federal Republic of Germany
Attn: Dr. E. Weitendorf
(Copy No. 66)

J. M. Voith Gmbh
Hydraulic Department
Postfach 1940
D-7920 Heidenheim
Federal Republic of Germany
Attn: Mr. Eichler
(Copy No. 67)

Applied Research Laboratory
The Pennsylvania State University
Post Office Box 30
State College, PA 16801
Attn: D. E. Thompson
(Copy No. 68)

Applied Research Laboratory
Attn: F. S. Archibald
(Copy No. 69)

Applied Research Laboratory
Attn: A. L. Treaster
(Copy No. 70)

Applied Research Laboratory
Attn: W. S. Gearhart
(Copy No. 71)

**DAT
FILM**

2